



universität
wien

MASTERARBEIT / MASTER'S THESIS

Titel der Masterarbeit / Title of the Master's Thesis

„Decarbonizing the Steel Industry:
How does a 100 % renewable powered steel production
influence electricity system structure and costs in Austria
and Germany? “

verfasst von / submitted by

Simon Büttner, B.Sc.

angestrebter akademischer Grad / in partial fulfilment of the requirements for the degree of
Master of Science (MSc)

Wien, 2023 / Vienna 2023

Studienkennzahl lt. Studienblatt /
degree programme code as it appears on
the student record sheet:

UA 066 299

Studienrichtung lt. Studienblatt /
degree programme as it appears on
the student record sheet:

Interdisziplinäres Masterstudium
Environmental Sciences

Betreut von / Supervisor:

Univ.-Prof. Dr. Thilo Hofmann

Contents

List of Abbreviations	iii
List of Figures	iv
List of Tables	iv
Abstract	1
Zusammenfassung	2
1 Introduction	3
2 Literature Review	5
2.1 Conventional Steel Production	5
2.1.1 Blast Furnace Route	6
2.1.2 DR - EAF Route	8
2.2 Decarbonizing Steel Production	9
2.2.1 Hydrogen-based Direct Iron Reduction	11
2.2.2 Electricity-based Iron Production	12
2.3 Integrating an Electrified Steel Production into the Energy System	13
3 Goals and Hypotheses	17
4 Methods and Data	18
4.1 Adapting the Power System Model <i>medea</i>	18
4.2 Modelling Approach	19
4.3 Data	21
4.3.1 Initial Capacities	21
4.3.2 Base Energy Demands	21
4.3.3 Energy Demand from <i>Iron Making</i>	22
4.3.4 Costs and Prices	23
5 Results	24
5.1 System Costs	24
5.2 Gross Electricity Consumption	27
5.3 H_2 Production and Imports	29
6 Discussion	30
6.1 Differences between AT and DE	30
6.2 The Role of Flexibility in DE	31
6.3 H_2 Imports and Domestic H_2 Production	33
6.4 Limitations	33
7 Conclusion	35
A Figures	41
B Notes	46

Acknowledgement

I would like to thank the numerous people who helped and accompanied me to complete this thesis. By now, it has been quite a journey from the first idea to the finished product - but finally the thesis is real! :D Unfortunately, I will not be able to name everyone who directly or indirectly helped me on this journey, so I will just name a few. If you actually read this thesis and your name is not below - be sure I am probably very grateful for your support, in whatever form you might have supported me! :) Of the people who I want to name I would particularly like to thank Sebastian Wehrle who was always a helpful support to understand the details of *medea* and Johannes Schmidt who was always a helpful, constructive and readily available supervisor. Both of them supervised me very well for this thesis even though they formally do not appear in the the official thesis documentation on the front page. Special thanks also go to Lisa who was a great support in our (often) weekly meetings to battle the great foe of procrastination and numerous other powerful enemies. Finally, I would like to give special props to me homie Ali(na) B who helped a lot in finding the numerous smaller and larger errors in the first draft of this thesis. To everyone else: thank you for small and large support and I hope you can enjoy reading this thesis! :D

List of Abbreviations

AEC	Alkaline Electrolyzer Cell
BF	Blast Furnace
BOF	Basic Oxygen Furnace
CCS	Carbon Capture and Storage
CCU	Carbon Capture and Utilization
CHP	Combined Heat and Power
DH	District Heating
DR	Direct Iron Ore Reduction
DRI	Direct Reduced Iron
EV	Electric Passenger Vehicle
EW	Electrowinning
FLH	Full Load Hours
GEC	Gross Electricity Consumption
GHG	Greenhouse Gas
H2DR	H_2 -based Direct Iron Ore Reduction
ha	Hectare
HBI	Hot Briquetted Iron
HP	Heat Pump
I & S	Iron and Steel
NG	Natural Gas
O & M	Operations and Maintenance
PV	Photovoltaic
RE	Renewable Energy
ror	Run-of-river
SOEC	Solid Oxide Electrolyzer Cell
TYNDP	Ten year network development plan

List of Figures

1	Schematic representation of a blast furnace	7
2	Schematic representation of a shaft furnace	9
3	Schematic representation of an electric arc furnace	10
4	Schematic H_2 -based steel production	11
5	Schematic molten iron oxide e	14
6	Overview of the modelled system	20
7	Total System Costs	24
8	System costs differences	25
9	Investment cost differences	26
10	Gross electricity consumption in AT and DE	27
11	Electricity generation from H_2 gas power plants	28
12	Domestic H_2 production in AT and DE	29
13	Comparison of electricity system flexibility in DE	32
A.1	System costs per country	41
A.2	Cost differences by cost type in AT	41
A.3	Cost differences by cost type in DE	42
A.4	Investment cost differences in AT	42
A.5	Investment cost differences in DE	43
A.6	H_2 imports into AT and DE	43
A.7	Average H_2 production over the course of one day	44

List of Tables

1	Initial Capacities	22
2	Crude Steel Production 2017 - 2021	23
3	Energy demand of electrolytic iron reduction	23
4	Technology Data	45

Decarbonizing the Steel Industry:

How does a 100 % renewable powered steel production influence electricity system structure and costs in Austria and Germany?

May 2023

Abstract

As energy systems need to be urgently decarbonized to meet climate protection targets, electricity systems must cope with the electrification of fossil-fuel powered processes. Simultaneously, they need to integrate increasing quantities of intermittent renewable electricity generation to achieve net zero greenhouse gas emissions. This poses an enormous challenge to existing electricity systems as they are designed for high shares of flexible fossil fuel based electricity generation. Operating completely renewable electricity systems, however, requires large flexibility to balance intermittent electricity generation with electricity demand without relying on readily available fossil fuels. In particular, electrifying large energy consumers such as the iron and steel (I & S) industry can therefore become a challenge for renewable electricity systems as they can fundamentally influence the operations of the electricity system. This study investigates the effects of directly or indirectly electrifying steel production on a completely renewable Austro-German electricity system. Thus, it represents an exploratory case study of how to successfully decarbonize the tightly coupled energy and industry sectors. The results indicate that flexibly-run H_2 electrolyzers, flexible H_2 gas power plants and utility-scale batteries will become crucial elements of a renewable electricity system in Germany in order to provide the necessary flexibility in the system to balance electricity generation and demand. In Austria, on the other hand, electrolyzers and H_2 gas power plants are likely not required as central elements of a completely renewable electricity system as Austria possesses sufficiently flexible hydro storage units that are even able to supply inflexible electricity consumers at times of low intermittent electricity generation. Furthermore, the results show that the cost and energy efficiency of using a technology in individual plants may differ to the overall system costs and system energy efficiency as supposedly cheap and more energy efficient technology might require additional infrastructure on a system level to function.

Zusammenfassung

Die Dekarbonisierung der Eisen- und Stahlindustrie stellt nationale Energiesysteme vor die Herausforderung große Mengen an treibhausgasneutraler Energie bereitstellen zu müssen, die ausschließlich aus erneuerbaren oder treibhausgasneutralen Energiequellen gewonnen werden dürfen. Eine derartige vollständige Dekarbonisierung des aktuell sehr kohlenstoffintensiven Hauptprozesses der Stahlerzeugung, der Eisenerzreduktions, kann nach derzeitigem Wissensstand nur über eine wasserstoffbasierte Eisenerzdirektreduktion oder über strombasierte Eisenerzelektrolyse erfolgen. Während die Produktion von grünem Wasserstoff erhebliche Energieverluste mit sich bringt und somit große Mengen erneuerbarem Strom benötigt, erfordert die strombasierte Eisenerzelektrolyse ausreichend verfügbaren Strom aus erneuerbaren Energiequellen. Dieser muss zudem praktisch jederzeit für die Stahlproduktion verfügbar sein, was das Stromsystem besonders in Zeiten geringer erneuerbarer Stromproduktion vor große Herausforderungen stellt. Die vorliegende Studie simuliert die Auswirkungen einer wasserstoffbasierten und einer strombasierten Eisenerzreduktion auf den Aufbau und die Kosten vollständig erneuerbarer Stromsysteme in Deutschland und Österreich. Dabei untersucht diese Studie die Auswirkungen verschiedener Ausbaubeschränkungen für Wind- und Solarenergie sowie die Auswirkungen verschiedener Wasserstoffimportpreise auf die jeweiligen Energiesysteme. Die Ergebnisse zeigen, dass Wasserstoffelektrolyseure im deutschen Stromsystem eine wichtige Rolle spielen werden, um Erzeugungsspitzen volatiler Stromerzeuger abzufangen und dass dadurch eine wasserstoffbasierte Stahlerzeugung kosten- und energieeffizient darstellbar ist. Eine strombasierte Stahlerzeugung würde in Deutschland hingegen die benötigten Kapazitäten teurer und ineffizienter Wasserstoffkraftwerke deutlich erhöhen, weshalb Eisenerzelektrolyse ein 100 % erneuerbares deutsches Stromsystem verteuern und sogar energieineffizienter machen würde. Das österreichische Stromsystem besitzt hingegen bereits große flexible Stromspeicherkapazitäten durch Wasserspeicherkraftwerke, weshalb Wasserstoffelektrolyseure keinen Zusatznutzen im Stromsystem erfüllen. In Österreich würde eine strombasierte Eisenerzreduktion daher die Kosten des Stromsystems reduzieren und gleichzeitig die Energieeffizienz des Stromsystems verbessern.

1 Introduction

Decarbonizing iron and steel (I & S) production to achieve climate protection goals represents an enormous challenge as the global I & S industry annually consumes about 8 % of global final energy use and produced about 7 % of the direct CO_2 emissions associated with energy use in 2019 (IEA, 2020). In 2015, 85 % of this final energy demand was provided by coal (Kim et al., 2022) to fire the numerous coke-based blast furnaces, which produce about 90 % of global primary steel (IEA, 2020). While primary steel production¹ represents the major steel production pathway, it is also eight to ten times more energy intensive as secondary² steel production (IEA, 2020). During primary steel production, *iron making* is by far the most energy- and carbon emission-intensive process as reducing iron ores (typically Fe_2O_3) to pure Fe requires large quantities of process energy and is typically realized with carbon as a reducing agent which produces large carbon emissions.

A complete decarbonization of I & S production³, therefore, requires to replace fossil fuels as both energy source and reducing agent with a carbon neutral process energy supply and with reducing agents that do not produce carbon emissions. While adaptations of conventional steel production processes allow considerable carbon emission reductions (Kim et al., 2022; Mousa, 2019), a complete decarbonization of primary steel production can only be achieved using new breakthrough technologies in the energy intensive *iron making* process. Venkataraman et al. (2022), for example, estimated the global carbon emissions of different combinations of steel production technologies and checked their compatibility with climate protection targets. They conclude that only a stark and rapid shift towards new zero-carbon steel production technologies can achieve carbon emission reduction in the global I & S industry compatible with emission trajectories to limit average global warming to well below 2° C. Harpprecht et al. (2022) performed a similar analysis for the transformation of the German I & S industry and estimate that not even their scenarios where zero-carbon technologies are deployed will be compatible with a 1.5° C target as existing *iron making* technologies and fossil fuel-based electricity production cannot be phased out sufficiently fast enough. They conclude that a successful decarbonization of the I & S industry will require a rapid decarbonization the electricity sector in combination with a rapid deployment of new zero carbon steel production technologies.

Hydrogen-based direct iron ore reduction (H2DR) represents the most prominent of such zero-carbon technologies to replace fossil fuels in *iron making*. In H2DR, H_2 replaces coal and other fossil fuels as both energy source and reducing agents during the reduction of iron ores and generates no process carbon emissions. When the H_2 that is used during H2DR originates from renewable electricity, H2DR is a completely carbon emission free process. Even though it is still considered a "new" breakthrough technology, H2DR is currently actively developed by various steel producing companies around the world. For example, the *HYBRIT* project in Sweden already operates a H2DR prototype furnace with a capacity of 1 ton Fe /hour and aims at increasing production capacity to 0.2 to 0.4 Mt direct reduced iron (DRI) per year after 2025 (Kushnir et al., 2020). In general, the process of H2DR-based *iron making* is related to the already established natural gas (NG) based direct iron ore reduction (Vogl et al., 2018). Despite the challenge of up-scaling H2DR, the currently biggest obstacle for a large-scale deployment of H2DR is the availability of green H_2 . In 2020, only 0.03 % (30 kt H_2) of global H_2 production were generated through water electrolysis (IEA, 2021). Consequently, sufficient quantities of green H_2 must first be produced before H2DR can fully replace fossil fuel-based steel production.

As an alternative to H2DR, iron oxide electrolysis represents an emerging breakthrough technology to produce carbon-free primary steel (Bailera et al., 2021; Cavaliere, 2019; Harpprecht et al., 2022; Venkataraman et al., 2022). In this process, iron oxides are reduced to metallic Fe

¹steel production from iron ores

²scrap-based

³While this text refers to "complete decarbonization" or "zero-carbon" technologies, the author of this study is aware that steel production will likely not be possible without any carbon emissions. Even though energy and energy carrier related emissions can be eliminated, certain process emissions will very likely persist. These include, for example, emissions from the erosion of the graphite electrodes in an electric arc furnace or from the use of lime, which inevitably generate CO_2 during its production. A complete decarbonization of steel production would therefore require either 100 % efficient carbon capture technologies or carbon emission offsets.

through an electric current either through the so-called electrowinning (EW) approach or in a process called molten oxide electrolysis (MOE). During EW, iron ores are placed in an alkaline solution at 110° C and accumulate as solid Fe at the cathode (Bailera et al., 2021). During MOE, iron ores are placed in a bath of molten electrolytes above the melting temperature of iron (1538°C), which produces molten Fe at the cathode of the iron ore electrolyzer (Cavaliere, 2019). Even though both iron oxide electrolysis technologies are not as far developed as H2DR, they could eliminate the intermediate step of producing large quantities of green H_2 for steel production. Like H2DR, iron ore electrolysis is currently actively developed in different projects around the world: Boston Metals, for example, aims at deploying commercial MOE plants already in the second half of this decade (Boston Metals, 2022b) while EW is researched for example by the EU-funded *Siderwin* project (Barberousse et al., 2020).

Switching the energy intensive steel production from fossil fuels to H2DR or iron oxide electrolysis, however, will pose a challenge for the underlying electricity system that needs to supply sufficient quantities of green H_2 or readily available renewable electricity for steel production. While H2DR-based *iron making* requires more H_2 -related infrastructure and might increase energy system costs and overall energy consumption, a large-scale deployment of iron oxide electrolysis would strongly increase direct electricity demand and might require larger energy storages and more flexible electricity generators in the electricity system. Due to the large energy consumption of the I & S industry, deploying either technology might therefore considerably affect the costs and the necessary set-up of the underlying electricity system, require different grid infrastructure and need very different grid expansion plans to prepare the urgently needed decarbonization of the I & S industry.

To the best knowledge of the author, no study has yet comprehensively investigated the effects of electricity- and H_2 -based I & S production on the electricity system to identify possible differences in electricity system set-up and costs. This is particularly important as the necessary renewable generation and grid infrastructure capacities for such energy-intensive projects need to be planned years ahead before new zero-carbon steel plants can commence operation (Kushnir et al., 2020). Accordingly, it is crucial to prepare the electricity system for the first near zero carbon steel production projects as early as possible to allow first breakthrough steel production technologies to commence operation when they are technologically mature around the end of the decade. Besides the direct emission reduction in steel production, an early adoption of first breakthrough steel technologies is also particularly valuable for the decarbonization of the global I & S industry as it can generate valuable spill-over effects for the global I & S industry (Pye et al., 2022).

To narrow the scope of this analysis, Austria (AT) and Germany (DE) were selected as suitable countries to assess the impacts of H2DR and electricity based steel production on the underlying electricity systems. The reasons are fourfold. Firstly, AT and DE both harbour a large I & S industries and represent the seventh- and first-largest steel producers in the EU (World Steel Association, 2022). While DE also constitutes the largest economy in Europe, steel production in AT is relatively large compared to the overall size of the Austrian economy. Secondly, AT and DE have both committed to build renewable electricity systems without relying on nuclear power plants (Deutscher Bundestag, 2022a; Österreichischer Nationalrat, 2021) but have very different conditions for renewable electricity systems. While AT is rich in water resources and contains relatively large hydro storage capacities, the German electricity system has historically been dominated by coal, gas and nuclear power plants and contains only little flexible renewable storage capacities. Accordingly, a renewable Austrian electricity system will be characterized by relatively large run-of-river (*ror*) and hydro storage power plants whereas a German renewable electricity system will primarily rely on wind and photovoltaic (PV) power plants that need to be complemented by new energy storage technologies. Thus, an assessment of AT and DE allows to compare the effects of large energy consumers on different types of renewable electricity systems. Thirdly, the Austrian and German electricity systems are well connected, which allows to partly account for flexibility in the overall system through international electricity exchange. Such flexibility is a central element of the European electricity system to stabilize the electricity system of countries with temporarily low generation. Finally, the present analysis could at the same time only be limited to AT and DE to keep computa-

tional requirements at an acceptable level while maintaining a sufficiently complex model that can represent real electricity systems.

The present paper, therefore, represents an exploratory study that investigates pathways towards a successful decarbonization of both the electricity system and the carbon emission intensive I & S industry. In particular, it analyzes not only the effects of H₂DR and iron ore electrolysis on the underlying electricity systems but extends its analysis to different scenarios how wind and PV capacities are expanded in AT and DE and investigates how different H_2 import prices affect renewable electricity systems. In this way, it considers a broad range of possible conditions for future electricity systems, which allows to draw conclusions on possible policies and grid expansion plans for a successful decarbonization of the respective electricity systems. Moreover, the results of this study will allow to assess the benefits and the feasibility of integrating a directly or an indirectly electrified I & S industry into completely renewable electricity systems. Furthermore, the results will help to evaluate the conditions under which domestic green H_2 production is able to compete with green H_2 imports from countries with better renewable resources.

The next section in this paper outlines the technological basics of breakthrough I & S production and discussed relevant literature on the decarbonization of steel production, which is followed by a short section on the goals and hypotheses of this thesis in chapter 3. Chapter 4 describes the scenarios, the modelling approach and the data that were used in the present analysis. Subsequently, chapter 5 outlines the insights into system costs, energy consumption and H_2 production produced by the model used in this study. The discussion chapter sets the results into the context of the different conditions for renewable electricity systems in AT and DE and highlights the role of different types of flexibility in the respective electricity systems. Finally, the discussion chapter also describes key limitations associated with the assumptions and the modelling approach taken in this study.

2 Literature Review

2.1 Conventional Steel Production

Steel production can be separated into a sequence of four steps: *raw material preparation*, *iron making*, *steel making* and *steel finishing* (Kim et al., 2022). After mining, iron ores (usually Fe_3O_3) are typically pre-processed through sintering or pelletizing before being reduced to raw iron (Fe) during *iron making*. The resulting Fe is then converted to crude steel along with iron and steel scraps during *steel making* and finally, transformed into finished steel products by casting and rolling during *steel finishing*. From all steps involved, *iron making* is by far the most energy intensive step consuming about 70 % of all energy used by the I & S industry (Kim et al., 2022). Consequently, decarbonizing *iron making* will provide a substantial contribution to meet climate protection targets considering that the I & S industry consumes about 8 % of the global final energy use and produces about 7 % of direct global CO_2 emissions from the energy sector (IEA, 2020).

Crude steel can be produced through the primary route, which is based on the processing of iron ores, and through the secondary route, where recycled I & S scraps are transformed to crude steel. Secondary steel production thereby consumes only one eighth of the energy as primary steel production since the processing of scraps requires only *steel making* and can skip the energy intensive step of *iron making* (IEA, 2020). In reality however, the distinction between primary and secondary steel production is not very clear-cut as scraps can be used alongside iron ore sourced Fe in several *iron and steel making* pathways. Therefore, primary and secondary steel production can be quantified by the share of I & S scraps used in the overall production process rather than through separate process steps. Since the shares of primary and secondary steel production strongly influence the overall energy consumption of crude steel production, they are an important parameter for this study as will be discussed in Section 4.3.3.

The following paragraphs provide a brief outline of conventional steel production routes, which is then followed by a description of possible options to decarbonize *iron making* through direct or indirect electrification.

2.1.1 Blast Furnace Route

The blast furnace-basic oxygen furnace (BF-BOF) route is by far the most important steel production technology being responsible for 90 % of global primary and about 70 % of total steel production in 2019 (IEA, 2020). It is separated into *iron making*, which occurs in a blast furnace (BF), and *steel making* in a basic oxygen furnace (BOF). Due to its high dependence on coal, producing steel through the BF-BOF route is very carbon intensive and results on average in 2.2 tons of CO_2 emissions per ton of crude steel (IEA, 2020). This includes 1.0 tons CO_2 in indirect emissions that arise from using non-renewable electricity and heat as well as from burning the carbon-rich BF off-gases for electricity production outside the *iron making* process.

In BFs, iron ore is simultaneously melted and reduced by coke and a stream of hot gases. While the exact chemistry of the BF reactions varies with the composition of the iron ore and the reaction gases, the following section describes the main steps in iron ore reduction in a BF (adapted from Hegemann and Guder (2019) unless stated otherwise). Since quite complex processes occur within BFs, only those processes that are relevant to understand the overall reaction mechanism are described here.

Figure 1 shows that the BF is fed from the top with solid input materials (iron ore, coke and additives), while hot reaction gases (a combination of oxygen, recirculated off-gases and carbon containing additives) enter the BF from the bottom part through injection tuyeres (turquoise in Figure 1). The solid materials sink towards the bottom and form a permeable layer (orange in Figure 1) for the reaction gas, which rises towards the top of the shaft. While the coke is burned by hot oxygen from the reaction gas, the iron ore is reduced to pure metallic iron (Fe) and at the same time melts as the temperatures exceeds the melting temperature of pure iron (1,538 °C). The liquid iron and other melted impurities in the iron ore flow through a layer of residual coke (so called "dead-man coke", dashed line in Figure 1) into the bottom of the BF forming layers of liquid slag and liquid iron (yellow areas in Figure 1), that can be separately extracted from the BF.

The reduction of the iron ore requires a gaseous reducing agent to efficiently access the iron oxides contained in the grained iron ore (Hegemann & Guder, 2019). This is achieved by burning coke (i.e. carbon) with hot oxygen (O_2 with temperatures above 1.000 °C) from the reaction gas. This reaction forms CO_2 and produces flame temperatures of up to 2.000 °C (Equation 1).



In the presence of carbon, however, CO_2 further reacts to CO in the endothermic Boudouard reaction (Equation 2). Due to the high temperatures in the BF, the equilibrium of the Boudouard reaction is strongly shifted towards the products (as it is an endothermic reaction with $\Delta H_{298} = +172.42 \text{ kJ/mol}$), so that virtually all CO_2 is immediately reconverted into CO .



The CO now acts as the gaseous reducing agent for the hematite (Fe_2O_3) in the iron ore to form magnetite (Fe_3O_4 , Equation 3). Again, the produced CO_2 is immediately reconverted into CO according to Equation 2. The CO now drives further reduction reactions, where magnetite is reduced to produce wüstite (FeO , Equation 4) and eventually to Fe (Equation 5). At temperatures above 1,000 °C, these reactions happen virtually at the same time as they are not kinetically limited. It therefore appears as if the coke directly reduces the iron ore. At temperature below 1,000 °C, e.g. in the upper part of the BF, Equation 2 is kinetically limited so that CO_2 is not immediately reconverted to CO and therefore cannot further drive

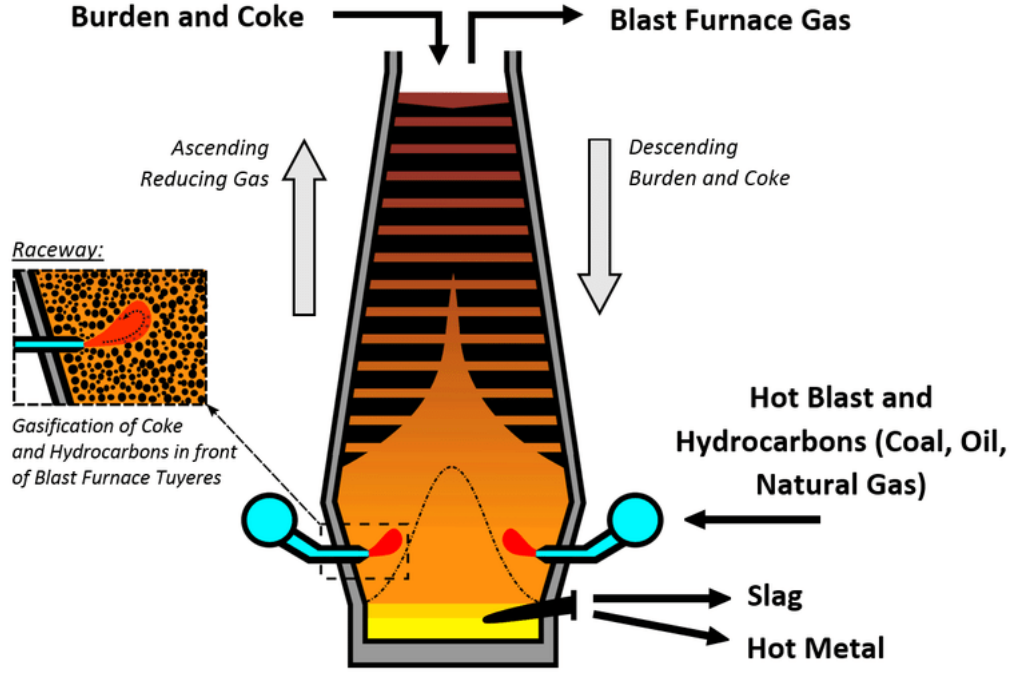
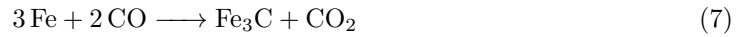
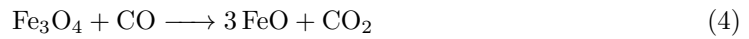


Figure 1: Schematic representation of a blast furnace. While solid materials are fed into the blast furnace from the top, hot reaction gases are blown into the furnace through Tuyeres (turquoise) in the bottom area. Orange area indicates agglomeration of solid materials (iron ore, coke, additives) and yellow area represents molten slag and iron that is collected at the very bottom of the furnace. Image from: Spanlang et al. (2016)

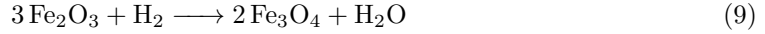
reduction reactions. Finally, Fe partly reacts with carbon to iron carbide (Fe_3C) (Equations 6 or 7), which is why the liquid Fe finally exits the BF with carbon content of 4-5 % (IEA, 2020).



The reduction of iron oxides into Fe can be aided by carbon and H_2 from other inputs than coke. H_2 can be either directly fed into the BF, or be formed in-situ from water vapour or and hydrocarbons that are fed into the BF as part of the reaction gas. Equation 8 shows the formation of H_2 and CO from water vapour and coke insides a BF. Consequently, this reaction does not only provide H_2 but also additional CO that can fuel the above mentioned reactions.



Similar to reactions 3 - 5, H_2 can perform every intermediate reduction step to transform hematite into Fe (Equations 9 - 11). This reaction cascade, however, can only continuously reform H_2 from the product H_2O in the presence of carbon as described in Equation 8.



Consequently, large quantities of CO and at cooler temperatures eventually CO_2 are formed during *iron making* in a BF. The carbon emission intensity of the BF can however, be considerably reduced by additives that introduce hydrocarbons or renewable biomass into the process (Mousa, 2019). These involve injecting pulverized coal, oil, natural gas, waste plastics or biomass into the BF with the reaction gases or mixing solid biomass with the coke loaded into the BF. Essentially, these additives replace carbon-based reduction reactions (Equations 3 - 5) with H_2 -based iron oxide reduction (Equations 9 - 11) as they contain more H_2 than pure coke. While this typically also reduces the costs of BF operation, coke cannot be entirely replaced by less carbon-intensive reducing agents as coke is essential for the mechanical stability inside the BF (Mousa, 2019). Therefore, BFs cannot be decarbonized beyond a certain threshold through low carbon materials or renewable carbon.

After *iron making* in a BF, the liquid Fe is directly fed into a BOF, where the iron is converted into crude steel. As a main process, oxygen is injected into the iron to reduce the carbon content of the iron to the desired level of typically below 1 % (IEA, 2020). The oxygen thereby serves as a reducing agent for the carbon the iron carbide and for other undesired impurities in the iron (Hegemann & Guder, 2020). Furthermore, other materials are added to the liquid Fe during *steel making* to alter the characteristics of the final steel product. The BOF produces also carbon emissions, yet only about 10 % of all CO_2 emissions from the BF-BOF route (Fan & Friedmann, 2021).

2.1.2 DR - EAF Route

The second most important route for steel production combines direct iron reduction (DR) for *iron making* and *steel making* in an electric arc furnace (EAF). While DR is only a minor pathway for primary steel production, the EAF represents the globally most important route for secondary steel production (IEA, 2020). About 28 % of global steel production stem from the DR-EAF route which includes the majority of secondary steel production (IEA, 2020). When EAFs are powered by renewable electricity, increasing the share of EAF-based *steel making* represents an effective way to partly decarbonize overall steel production. The following section outlines the chemical and technical principles of the Midrex DR technology, which currently dominates global DR production (Bailera et al., 2021), and the main process in an EAF.

DR is typically performed in shaft furnaces, where iron ore is reduced to Fe in a solid state. Like BFs, DR shaft furnaces are counter-current furnaces, where solid iron oxide is fed into the furnace from the top and moves opposite to the reaction gas flow as indicated in Figure 2 (red arrows for solid material, blue arrows for gas). A shaft furnace is split into three parts: an upper section where the iron oxide reduction reactions occur, a bottom section where the reduced iron is cooled and a middle section separating reduction reaction and cooling (Hamadeh et al., 2018). Since the iron oxides are not melted in the process, they need to be fed into the DR furnace as pellets composed of compressed grains to ensure that the reaction gases can sufficiently access the iron oxides in the iron ore. The reaction gas itself is primarily composed of a mixture of CO and H_2 , which are produced by methane steam reforming (Hamadeh et al., 2018). Injected with a temperature of around 900 °C, these gases reduce the iron oxides according to Equations 3 - 5 and Equations 9 - 11, thereby producing so-called "sponge iron" with a typical carbon content of 1 - 2.5 % (Hegemann & Guder, 2019). Overall, the reaction from Fe_2O_3 to Fe is endothermic and therefore requires heat energy to proceed (Pei et al., 2020). This heat can be partly recovered by cooling the grains at the bottom part of the furnace with methane that is thereby preheated for steam reforming (Hamadeh et al., 2018).

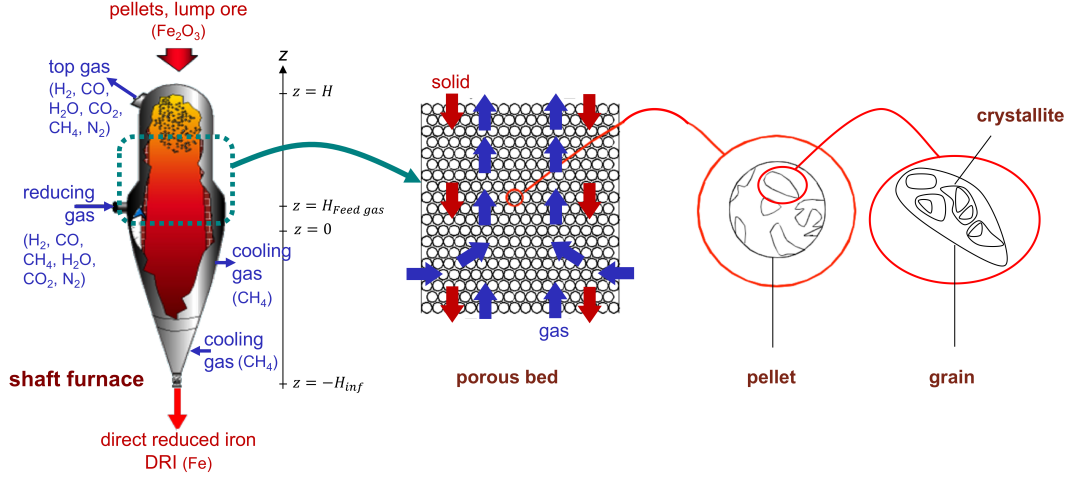


Figure 2: Schematic representation of a shaft furnace for natural gas based direct iron reduction. The image on the very left shows the general shape of the furnace as well as the composition of the most important material inputs. The images in the middle and on the right depict the granular structure of the solid materials at increasingly spatial resolution. In the middle, the red arrows indicate the flow direction of solid materials from top to bottom while the blue arrows indicate the flow direction of the ascending reaction gas. Image from: Hamadeh et al. (2018)

Since the direct-reduced iron (DRI) produced in a DR furnace is unstable over longer time periods and can be oxidized or spontaneously self-ignite, DRI needs to be converted to hot briquetted iron (HBI) before storage or transport (Pimm et al., 2021). Alternatively, the cooled DRI pellets can be transported over short distances for further on-site processing in a EAF.

An EAF is a cylindrical furnace equipped with one to three graphite electrodes that provide the energy for melting and refining a mixture of I & S scraps, HBI or granular DRI into crude steel. Figure 3 shows the typical structure of an EAF, which follows four phases: *charging*, *melting*, *refining* and *tapping* (Hay et al., 2021). During *charging*, the iron mixture is loaded into the furnace, after which they are melted through an electric arc generated by the graphite electrode(s) in the center of the EAF. This *melting* process can be assisted by oxyfuel burners fed with natural gas or oil (Bailera et al., 2021; Hay et al., 2021). Similar to the processes in a BOF, the liquid *Fe* is then refined by adding oxygen and other materials to remove impurities and excess carbon to adjust the characteristics of the produced steel (*refining*). It is sometime even necessary to add carbon into the liquid *Fe* when the input *Fe* contains only little carbon (Hay et al., 2021). Finally, the liquid crude iron is released from the EAF for casting and further processing in the *tapping* phase.

EAFs constitute a *steel making* technology with near zero CO_2 emissions when powered by renewable electricity and zero-carbon input materials. According to IEA (2020), 100 % scrap-fed EAFs produce only about 0.04 tons of direct CO_2 emissions per ton of crude steel, which originate from the use of fossil fuels in oxyfuel burners and from the erosion of the graphite electrodes. If EAFs operate entirely on renewable electricity, they produce no further indirect CO_2 emissions. Consequently, scrap-based steel production in EAFs produces less than 4 % of the CO_2 emissions from the DRI-EAF route and less than 2 % of the CO_2 emissions of the BF-BOF route (IEA, 2020). If EAFs can be fed with other CO_2 emission free input materials than scraps, I & S production can essentially become carbon neutral.

2.2 Decarbonizing Steel Production

Even though considerable carbon emissions reductions can be achieved with conventional steel production technologies, a (near) complete decarbonization of steel production is only possible

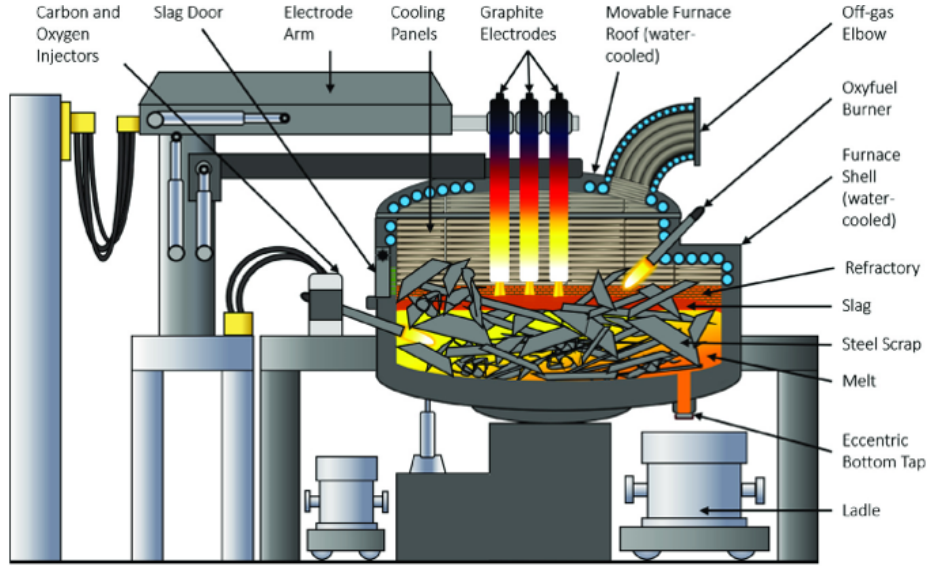


Figure 3: Schematic representation of an electric arc furnace (EAF). The image shows an EAF with three graphite electrodes at the center, which provide the energy to melt and convert the Fe to molten crude steel. During the process, carbon oxygen and other additives can be fed into the liquid Fe to depending on the desired characteristics of the final steel product. Image from: Hay et al. (2021)

through large-scale electrification of *iron making* and *steel making*. While carbon emissions from BF's can be partly reduced by substituting coke with less-carbon intensive energy carriers (Mousa, 2019), Venkataraman et al. (2022) show that upgrading all existing conventional BF's to the best-available technology until 2060 only slightly reduces emissions due to an expected increase in global steel demand. They further demonstrate that only a large-scale deployment of zero emission technologies such as H_2 -based direct iron ore reduction (H2DR) or electrowinning (EW) achieves sufficient emission reductions in the global I & S industry to remain well below a carbon budget compatible with the $2^\circ C$ goal. Similarly, Fishedick et al. (2014) assessed the long-term economic viability of H2DR and EW in Germany compared to conventional steel production incorporating carbon capture and storage (CCS) and found that emission reduction below 80 % of 1990 levels are not possible in the I & S industry without H_2 or electricity based iron ore reduction technologies. They also predict H_2 -based production to become the best investment choice of all considered technologies after 2040, while electricity-based steel production becomes the most energy efficient technology and could become economically attractive in a 100 % renewable energy system with low electricity prices.

CCS or carbon capture and utilization (CCU) technologies, on the other hand, will likely not allow near zero carbon steel production but rather become an intermediate technology to reduce emissions during a transition phase towards H2DR and direct electrification of steel production. Gielen et al. (2020), for example, state that CCS technologies are unlikely to become dominant in the I & S industry due to high costs and stagnating progress in CCS technology development. And indeed, CCS and CCUS technologies are currently not able to remove all carbon emissions from BF's and therefore lead to insufficient long-term emissions reductions (Fishedick et al., 2014; Harpprecht et al., 2022; Venkataraman et al., 2022). Accordingly, CCU and CCS might serve as an intermediate solution to abate carbon emissions from existing conventional steel production technologies to keep transition pathways compatible with climate protection targets (Harpprecht et al., 2022), in particular when ambitious targets such as the $1.5^\circ C$ goal must be reached (Victoria et al., 2022).

A long term (near) complete decarbonization of steel production can therefore only be achieved through new H_2 - and electricity-based steel production technologies. These technolo-

gies, however, are as of now not fully developed to be commercially available and are currently at different stages of their technical development. Therefore, they can only serve as a long-term substitution of existing fossil-fuel based infrastructure (IEA, 2020; Kim et al., 2022). The following sections provides a summary of the relevant H_2 -based and electricity-based steel production technologies that might become commercially available to replace fossil fuel based steel production technologies.

2.2.1 Hydrogen-based Direct Iron Reduction

For *iron making*, H_2 can be used during steel production to replace fossil fuels as an energy carrier and reducing agent through a process termed H_2 -based direct iron ore reduction (H2DR). This section outlines the main principles of H2DR technology *iron making*, which is very similar to the Midrex DR process described in Section 2.1.2. Figure 4 shows the main components involved in the H2DR process set-up as described by Vogl et al. (2018). Like in NG-based DR, the main unit is a counter-current shaft furnace, where iron ore pellets are fed into the furnace from the top and slowly move towards the bottom of the furnace. In contrast to NG-based DR, H_2 is fed as the reaction gas into the furnace in the lower part of the furnace and reduces the downwards moving iron ore pellets at temperatures between 700°C - 900°C according to Equations 9 - 11 (Bhaskar et al., 2020). Since these temperatures are below the melting temperature of metallic Fe , H2DR produces solid DRI pellets like those produced in NG-based DR.

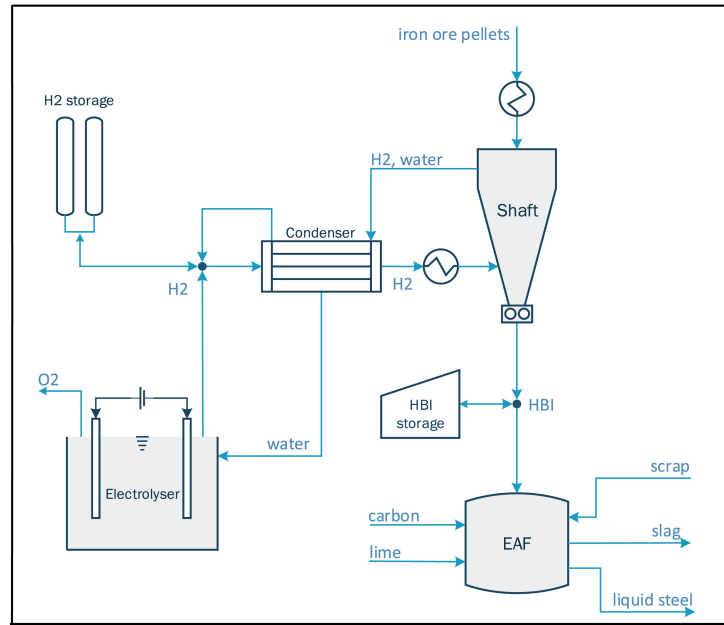


Figure 4: Schematic system set-up for green H_2 -based steel production. H_2 is produced from renewable electricity in an electrolyzer and then fed into a H_2 shaft furnace to reduce iron ore. The produced water vapour can be recycled in an electrolyzer to reform H_2 , while the reduced Fe can either be stored as HBI or directly converted to crude steel in an EAF. Image from: Vogl et al. (2018)

Since the *iron making* process requires carbon-free H_2 to become (near) carbon neutral, the H_2 for the reaction needs to be produced via water electrolysis powered by renewable or nuclear energy. Like NG-based DR, the reduction of iron ore through H_2 is endothermic and operates at temperature above 700°C , and therefore requires additional heat energy to proceed. For this, iron ore and H_2 are preheated before they are injected into the shaft furnace (symbolized by the round symbols with a zigzag line in Figure 4), which requires about 600 kWh of electricity per ton of produced DRI (Bhaskar et al., 2020). This already considers waste heat recycling in

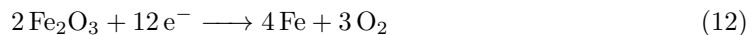
a condenser, which separates excess H_2 from the water vapour in the exhaust reaction gases to further recycle them. The excess H_2 can then be recirculated through the shaft furnace, while the waste H_2O can be fed into an electrolyzer to produce further H_2 . After successful reduction in the shaft furnace, the DRI pellets can either be directly used in an EAF or be converted into HBI for storage and transport. Compared to the traditional BF-BOF route, DR routes allow to decouple *iron making* from *steel making*, which can notably affect spatial and temporal steel production strategies (Gielen et al., 2020; Toktarova et al., 2022; Vogl et al., 2018) as will be discussed in Section 2.3.

On a small scale, DR reactions of solid iron ore can be described through a "shrinking core" model (Bhaskar et al., 2020), where the reaction gas (here H_2) first adsorbs and then diffuses into the iron ore grains. The subsequent step by step reaction of the reaction gas with the iron ore creates layers of iron in different oxidation states within each iron ore grain, where the outermost layers contain iron in the most reduced state. As the reduction reaction continues, the outmost layer containing pure Fe spreads to the center of each grain until the entire grain is reduced. The water vapour produced in each reduction reaction subsequently desorbs from the grains and is transported away within the gas stream in the furnace. Since the transport rates of H_2 and H_2O are the limiting factor of the reaction, the size and porosity of the iron ore pellets strongly influences overall reaction rates (Bhaskar et al., 2020). Furthermore, injecting more H_2 than strictly necessary for complete iron ore reduction accelerates reaction times even though it also increases overall energy consumption (Vogl et al., 2018).

Even though the chemical and technical processes for H2DR are well known, it is still a technology under development and not ready for full-scale industrial deployment. While the first commercial purely H_2 -based DR furnace started operation already in 1999, it was based on a different technological process and was not economically unsuccessful, so operations had to terminate prematurely (Bailera et al., 2021). Accordingly, there is currently no industrial-scale H_2 -based steel production facility operating in the world. On the technological readiness scale, H2DR is being considered to have reached level 5, for which the operation of a large scale prototype is a prerequisite (IEA, 2020). Such a prototype was built in Sweden with a capacity of 1 t of DRI per hour as part of the HYBRIT project that intends to fully decarbonize Sweden's steel production through H2DR-EAF technology by 2045 (Kushnir et al., 2020). Over the coming years, the existing pilot plant is planned to be upgraded to an industrial-scale H2DR demonstration plant with a capacity between 0.2 and 0.4 Mt DRI per year after 2025 and eventually to a full-scale H2DR-EAF facility producing 1.5 Mt of crude steel per year in 2040 (Kushnir et al., 2020). The HYBRIT program in Sweden is, however, not the only project which aims to test industrial scale H2DR as other projects in Germany (SALCOS, Midrex plant for ArcelorMittal), Austria (SuSteel), France (ULCOS) and the United States (flash iron making) show (Gielen et al., 2020).

2.2.2 Electricity-based Iron Production

Another possibility to replace fossil fuels as energy carrier and reducing agent for steel production is to directly use electricity for *iron making*. Instead of reducing solid iron ore pellets like in H2DR, this route places iron ores in an electrolytic bath, where an electric current provides the required electrons and energy for the reduction reaction. The concept of ore electrolysis is already commercially available for the production of aluminum (Cavaliere, 2019), lead, copper, rare-elements as well as for processing specific iron ores (Venkataraman et al., 2022). For the production of metallic Fe , two different electrolytic processes are possible: (1) electrowinning (EW), where iron ore particles are suspended in alkaline solution and electrolysis is performed at temperatures around 110°C (Bailera et al., 2021); and (2) molten iron oxide electrolysis (MOE), where iron oxides are molten and reduced in a bath of electrolytes at temperatures above 1538°C (Cavaliere, 2019). The overall reduction reaction for both EW and MOE is shown by Equation 12.



The EW process is described in detail by Cavaliere (2019) and is summarized in the following paragraph. First, fine solid iron ore particles (Fe_2O_3) are suspended in a hot and highly concentrated aqueous $NaOH$ solution with a temperature between $90^\circ C$ - $110^\circ C$. Second, applying a current to the solution allows to form solid Fe and hydroxide ions (OH^-) from the iron ore at the cathode. While the hydroxide ions remain in solution and can move to the anode, the Fe form a solid conducting layer on the surface of the cathode that allows the reaction to further progress. At the same time, O_2 is produced from OH^- at the anode. Finally, the solid metallic Fe deposit on the cathode can be removed and fed into an EAF for further processing.

Even though the principles of EW have already been successfully demonstrated, for example by Allanore et al. (2010) or in a pilot plant of the Siderwin project (Harpprecht et al., 2022), challenges for EW include the up-scaling of the process to produce industrial-scale quantities of Fe while maintaining high efficiencies (Cavaliere, 2019). If these challenges are overcome, EW has the potential to directly electrify *iron making* with estimated electricity demands between approximately 2.7 MWh (Barberousse et al., 2020) and 3.1 MWh (Cavaliere, 2019) per ton of produced Fe . According to Barberousse et al. (2020), EW electrolyzers could also constitute flexible energy consumers that help to bridge gaps between renewable electricity generation and electricity demand.

While EW requires only temperatures around $100^\circ C$, MOE allows to produce molten metallic Fe from electricity at temperatures above $1600^\circ C$. MOE is a technology related to the already established Hall-Heroult process for aluminum reduction only that it operates at a higher temperature to exceed the melting temperature of Fe (Venkataraman et al., 2022). In MOE, an electric current first melts the iron ore and accompanying electrolytes to produce molten Fe and gaseous O_2 according to the overall reaction shown by Equation 12. One of the furthest developed concepts for MOE comes from the company Boston Metals which develops modular MOE electrolyzers that can be combined to industrial scale steel production facilities according to their website (Boston Metals, 2022a). Figure 5 shows a MOE electrolyzer module as presented by Boston Metals (2022b). It consists of a stationary cathode at the bottom and a movable inert anode that is lowered into the electrolyzer from the top. The iron ore is fed into the electrolyzer together with the electrolyte from the top. After successful melting and iron reduction, the reduced molten Fe accumulates at the bottom of the electrolyzer and forms a liquid cathode. Finally, the liquid Fe can be tapped and directly fed into an EAF, where no further energy is required for melting the Fe . While Boston Metals is currently still developing their MOE electrolyzer cell, they intend to construct a demonstration plant by 2025 (Boston Metals, 2022b). Despite its similarity to already established metal oxide electrolysis processes, the development of MOE has so far been slow due to (1) difficulties with finding a suitable and affordable anode material that can withstand the extreme conditions at the anode with temperatures above $1538^\circ C$ and simultaneous oxygen evolution (Venkataraman et al., 2022) and (2) the various possible valence states of Fe ions in the electrolyte melt, which reduce overall process efficiency (Wiencke et al., 2018). Nevertheless, previous research indicates that suitable anode materials exist for MOE (Allanore et al., 2013) and the production of liquid Fe through MOE has already been successfully demonstrated in lab scale reactors (Wiencke et al., 2018).

2.3 Integrating an Electrified Steel Production into the Energy System

Electrifying the I & S industry through electrolytic or H_2 -based *iron making* significantly increases electricity and H_2 demands and thereby represents a challenge for energy systems. Pimm et al. (2021), for example, estimated that producing 1 Mt of crude steel per year from iron ore through the H2DR-EAF route would translate into continuous demands of almost 200 MW H_2 and 71 MW electricity, excluding the electricity demand for electrolytic H_2 production. Similarly, Harpprecht et al. (2022) analyzed different decarbonization pathways of the German I & S industry including a combination of H2DR-EAF and EW-EAF routes and estimate that additional 83 - 87 TWh electricity will be needed for a decarbonized I & S production in DE in 2050, of which almost 32.7 TWh will be required to produce 24.4 TWh H_2 for H2DR. Other studies predict an even higher H_2 demand in DE reaching 36 TWh (Prognos, Öko-Institut and

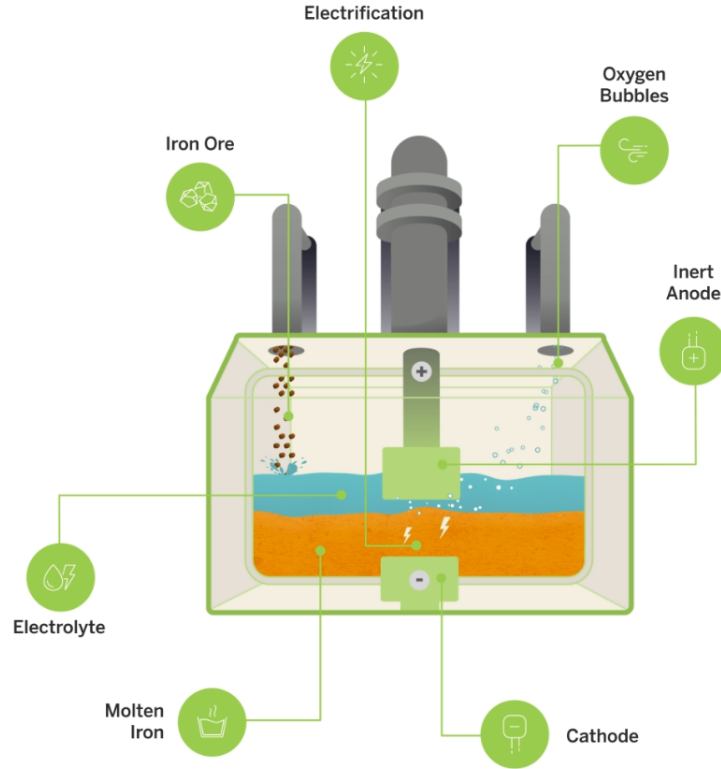


Figure 5: Schematic representation of a molten iron oxide (MOE) electrolyzer module as presented by the company Boston Metals. Image from: Boston Metals (2022b)

Wuppertal Institut, 2021) or even 80 TWh (BMWK, 2020) H_2 per year for I & S production only. For AT, the Austrian National Hydrogen Strategy expects a H_2 demand of 10.8 TWh/year solely for H2DR (BMK, 2022).

Producing such quantities of green H_2 requires even higher amounts of domestic renewable electricity and large volumes of water unless green H_2 can be imported in considerable quantities. With electrolyzer efficiencies expected to reach 70 - 75 % in 2050, producing 1 TWh H_2 will require 1.33 -1.43 TWh electricity and around 270.000 m^3 of water (Danish Energy Agency, 2022b). Accordingly, switching *iron making* to H2DR requires a massive expansion of electrolyzer and RE capacities. While only about 0.12 GW of electrolyzers were installed in whole Europe in 2020 (IEA, 2021), the National H_2 Strategies of AT (BMK, 2022) and DE (BMWK, 2020) target minimum electrolyzer capacities of 1 GW in AT in 2030 and 10 GW in DE in 2040. Other studies, however, suggest that these target capacities considerably underestimate the required electrolyzer capacities. Ramsebner and Haas (2021), for example, calculate that 4 GW electrolyzer capacity might be needed in AT by 2040 solely to produce the H_2 used in H_2 power plants to balance intermittent renewable generation. In DE, studies by enervis (Stiftung Arbeit und Umwelt der IG BCE, 2021) and Fraunhofer ISI et al. (2021) expect electrolyzer capacities in 2040 to range between 35 - 50 GW and 10 - 37 GW respectively, whereas Harpprecht et al. (2022) state that at least 7.2 GW electrolyzers are necessary to only cover H_2 demand for steel production.

While H_2 -based steel production only indirectly increases electricity demands, electrolysis-based *iron making* directly increases electricity demand significantly. For MOE, Boston Metals expects an electricity consumption of 4 MWh per ton of crude steel over the entire crude steel production process (i.e. *raw material preparation, iron making and steel making* (Fan & Friedmann, 2021). For EW, Barberousse et al. (2020) computed additional annual electricity

demands of 32.8 TWh in AT and 140.5 TWh in DE in 2050, if primary steel production grew by 0.8 % per year and was entirely based on EW. While their values include the electricity demand for the entire crude steel production process from *raw material preparation* to *steel making*, the EW process alone (2,72 MWh/ t_{steel}) would add 24.8 TWh (AT) and 106.1 TWh (DE) to the annual electricity demand in 2050. Even though these numbers appear very large, they might still be considerably lower than the overall electricity demands if H_2 for H2DR were produced domestically and at least 25 % of the electricity used for H_2 production would be lost during electrolysis.

Compared to a final electricity consumption of 63.5 TWh in AT (Statistik Austria, 2022) and 499.9 TWh in DE (AG Energiebilanzen, 2021) in 2019, all the above mentioned energy demands for a directly or indirectly electrified I & S production represent huge additional demands for the Austrian and Germany electricity grids. Even though the exact energy requirements for H2DR and EW vary considerably in the literature (see Section 4.3.3 for a further discussion), the above mentioned numbers indicate that a large energy infrastructure expansion will be necessary to decarbonize steel production. In addition, steel production typically follows rather constant production rates as plant operators need to achieve high plant utilization rates for profitable production (Toktarova et al., 2022). This adds a constant energy demand to the system while electricity is mostly generated by intermittent RE technologies. Consequently, decarbonizing steel production might increase energy storage demands and require a careful optimization of the RE generation mix, for example, through an optimization of the ratio between wind and PV capacities as suggested by Pimm et al. (2021).

A direct or indirect electrification of steel production might, however, not only change the required electricity supply but also introduce flexibility in the steel production process. Firstly, H2DR-based steel production allows to decouple electricity consumption for H_2 production and H_2 use in *iron making* as H_2 can be stored before use in a H2DR furnace. Secondly, solid DRI can be stored and transported as HBI and be fed into an EAF at times and locations where cheap electricity is available (Pimm et al., 2021; Toktarova et al., 2022; Vogl et al., 2018). Furthermore, EAFs operate in batch mode and can therefore, introduce some degree of flexibility into *steel making* (Vogl et al., 2018). Toktarova et al. (2022) analyzed flexible steel production in detail through a linear cost-optimization model with the goal to identify ideal investment decisions for H2DR-based steel production and electricity generation in central and northern Europe. They found that over-investments in H2DR steel production assets as well as in H_2 and HBI storages are cost-efficient as this allows to align steel production with the availability of cheap renewable electricity. They further highlight that steel production and in particular *iron making* capacities will likely be centered in regions where cheap and abundant renewable electricity is available. This indicates that more flexible steel production and a separation of *iron making* from *steel making* is a realistic possibility in the future. Furthermore, their results indicate that renewable electricity generation is economically more attractive than electricity generation from nuclear power plants or even NG-power plants if they need to compensate their CO_2 emissions. Similar to the findings of Toktarova et al. (2022), other studies support the conclusion that H2DR will likely allow and incentivise a more flexible steel production (Bailera et al., 2021; Lechtenböhmer et al., 2016; Vogl et al., 2018).

Iron ore electrolysis technologies might also allow flexible steel production. Barberousse et al. (2020), for example, suggest that a direct electrification of *iron making* through EW could provide demand-side flexibility similar to the way how already established electrolysis processes can operate flexibly. They support this statement by the suggestion that low-temperature iron ore electrolyzers do not require long start-up or cool-down times. Furthermore, EW produces Fe that can be converted to HBI and therefore be further processed at other times or places with better availability of cheap electricity. Nevertheless, these arguments for a flexible steel production through EW do not consider the economics of a steel production plant, which typically try to optimize plant utilization rates. For MOE, it is uncertain to which degree it might be able to operate flexibly as it requires high temperatures and therefore long start-up times. Yet, Boston Metals advertise that the modular structure of their MOE technology allows to use exactly the amount of MOE electrolyzers as desired in a facility (Boston Metals, 2022a).

This might allow to vary the number of active MOE electrolyzers according to the availability of cheap electricity.

Within the large number of energy system modelling publications, few studies fully assess the effects of a wide-spread electrification of multiple sectors on the energy system with high time resolution and with a detailed representation of I & S production. As already mentioned above, Toktarova et al. (2022) explicitly investigate the specific interactions of H2DR-based steel production and local energy systems to derive conclusions on where and how the I & S industry can operate economically efficient in the future. Nevertheless, they do not consider increased electricity demands from the electrification of other sectors into their analysis and model the energy system only in 12 hours time steps, which neglects small scale variations in energy supply and demand and cannot accurately reflect short-term energy storage requirements. Victoria et al. (2022), on the other hand, used the comprehensive open Py-PSA model to evaluate transition pathways for the energy sector that limit carbon emissions from 37 European regions according to carbon budgets associated with goals to limit global warming to 1.5°C - 2°C. While they use a rather high time resolution of 3h and explicitly model the required grid capacities for a large-scale expansion of RE, they only consider energy demand for steel production from H2DR, assume a very high scrap share of 70 % and do not discuss the implications of electrifying steel production on the electricity system.

Pimm et al. (2021) and Harpprecht et al. (2022) go further and explicitly address the issue of providing the energy system infrastructure required to support steel production through H2DR. Pimm et al. (2021) use a linear cost optimization model to determine the most cost-efficient structure of the UK energy system for a H2DR-based steel production until 2040. While they use data with 1h resolution, they aggregate each month of a year into one representative day to reduce computation requirements. With that, they fail to accurately represent daily variability of RE generation, for example, at individual days with low wind and solar resources. On the other hand, their model allows a considerable degree of flexibility in the energy system through H_2 and electricity storage, through HBI imports in steel production as well as through electricity production from H_2 gas expansion turbines. Harpprecht et al. (2022) explore pathways to decarbonize the German I & S industry that are compatible with carbon budgets for limiting global warming to 1.5°C and 1.75°C. They provide an in-depth evaluation of energy consumption and the associated CO_2 emissions of various transformation pathways including both H2DR and EW. Yet, they do not model the underlying energy system but only provide a rough estimation of how much additional RE and electrolyzer capacities will be required to electrify German steel production. Thereby, they do not neither consider the economics of expanding the energy system nor the required energy storage to balance electricity supply and demand.

To the best knowledge of the author, no study has yet directly compared the energy system effects of electricity- and H_2 -based I & S production at high temporal resolution. While some studies (Harpprecht et al., 2022; Venkataraman et al., 2022) considered EW as a possible *iron making* technology in their scenarios, only Mayer et al. (2019) constructed separate scenarios for a H_2 -based and electricity-based steel production. However, they use the electricity-based scenario only to evaluate the macroeconomic effects of low electricity prices in steel production and do not directly compare electricity-based and H_2 -based steel production scenarios. In addition, their electricity-based *iron making* scenario is based on the hybrid H_2 -plasma direct steel production technology, which is a mixture of H_2 -based and electricity-based steel production and also still at an early stage of its technological development. This thesis can, therefore, complement the existing literature by providing a detailed evaluation of the effects of either H_2 -based or electricity-based *iron making* on the energy system at a high temporal resolution. It can further refine predictions about the effects of a decarbonized I & S industry on the energy system by considering additional electricity demands from the electrification of other sectors and by accounting for energy storage requirements as well as grid stabilizing services. Even though both H_2 -based and electricity-based *iron making* technologies might not reach technological maturity in the coming years, their implementation into the electricity grid needs to be planned far ahead (Kushnir et al., 2020) and successful early movers can create valuable spill-over effects to accelerate the global transformation of the I & S industry (Pye et al., 2022).

3 Goals and Hypotheses

The goal of this thesis is to simulate the effects of a direct and indirect electrification of *iron making* on 100 % renewable electricity systems in AT and DE using the power system model *medea*, which was developed by Wehrle et al. (2021). This thesis was designed as an exploratory study that captures different aspects of mature renewable electricity systems and asks the following research questions:

- How does a direct electrification of steel production change electricity system costs, energy storage requirements and H_2 use in AT and DE compared to H_2 -based steel production?
- How do capacity expansion constraints on onshore wind and PV affect system costs, energy storage requirements and hydrogen imports in AT and DE?
- How sensitive are the Austrian and German electricity systems to H_2 import price changes?

This thesis, therefore, attempts to analyze renewable electricity systems under scenarios with different assumptions on (1) the steel production technology, (2) wind and PV capacity constraints, and (3) H_2 import prices. Consequently, the main goal of this thesis is to explore how the Austrian and German electricity systems behave under different possible future scenarios and to derive similarities and differences between the two renewable electricity systems. In particular, this study aims at identifying the relevance and the approximate required capacities of different key elements in those renewable electricity systems, such as storage units. Furthermore, another focus of this study is to evaluate the role of domestic H_2 production in different renewable electricity system. Finally, this thesis attempts to provide data for future decisions on the role of different technologies in steel production and to provide a basis to better judge the effects of replacing fossil fuels with direct or indirect electrification technologies in energy-intensive applications.

The following hypotheses are formulated for this thesis:

1. Electricity-based *iron making* reduces overall energy system costs compared to H_2 -based *iron making*.

Since a direct electrification of the I & S industry does not require additional H_2 infrastructure, scenarios with electricity-based *iron making* result in overall lower system costs. This hypothesis assumes that the required additional infrastructure for a sufficient H_2 supply is more costly than the potentially required additional infrastructure for an elevated electricity supply to the I & S industry. The corresponding alternative hypothesis can be formulated as: Electricity-based *iron making* does not reduce overall energy system costs compared to H_2 -based *iron making*.

2. Electricity-based *iron making* lowers the gross electricity consumption in the electricity system compared to H_2 -based *iron making*.

As will be discussed in chapter 4.3.3, electricity-based *iron making* is herein assumed to be less energy intensive than H_2 -based *iron making* when considering the electricity that is required to produce green H_2 . We therefore, expect that the lower gross electricity demand from electricity-based *iron making* also translates into a lower gross electricity consumption in the overall system. Accordingly, this assumes that possible system effects such as higher battery storage losses do not compensate the additional energy losses in H_2 -based *iron making*. The alternative hypothesis can be formulated as: Even though electricity-based *iron making* requires less electricity than H_2 -based *iron making*, it does not lower gross electricity consumption in the overall electricity system.

3. Lower H_2 import prices reduce overall system costs in all scenarios and reduce system costs over-proportionally for scenarios with H_2 -based *iron making*.

Green H_2 import prices will affect overall system costs as soon as they are lower than the marginal production costs for domestic green H_2 production as it will be economically better to import green H_2 than to produce it in the domestic electricity system.

In these cases, overall system costs will fall with lower H_2 import prices. Accordingly, this hypothesis assumes that H_2 imports can economically (out)compete (with) domestic green H_2 production at all considered H_2 import price ranges. Lower H_2 import prices will therefore, also reduce overall system costs. Since overall H_2 demand is higher in scenarios with H_2 -based *iron making*, the system costs decrease stronger in these scenarios than in scenarios with electricity-based *iron making*. A strong over-proportional decrease in system costs in the H_2 scenarios compared to the *electricity scenarios* could therefore, even partly refute the hypotheses 1 at very low H_2 import prices. The corresponding alternative hypotheses can be formulated as: (a) Lower H_2 import prices do not reduce overall system costs in all scenarios and (b) lower H_2 import prices do not over-proportionally reduce system costs in scenarios with H_2 -based *iron making* than in scenarios with electricity-based *iron making*.

4 Methods and Data

4.1 Adapting the Power System Model *medea*

The power system *medea* (Wehrle et al., 2021) was chosen for the purpose of this study as it can endogenously optimize installed energy generation, storage and exchange capacities under given restrictions with the goal to minimize overall system costs. Thus, it allows to explore the optimal energy system set-up under exogenously determinable restrictions such as constraints on energy demands or generation capacities. *medea* operates in discrete time steps, in each of which it balances energy supply and demand and thereby mimics functioning energy markets. This allows to simulate the interactions of intermittent electricity generation and thereby to capture short-term dynamics of an electricity system. Furthermore, *medea* allows to integrate exogenous demands of different energy carriers into the modelled system, which can be coupled through co-generation units or through technologies that convert one energy carrier into another. Consequently, *medea* can simulate highly coupled energy systems, where the supply of different final energy carrier demands can be endogenously optimized through different possible technologies. Finally, *medea* also includes a requirement that sufficient flexible technologies must be active in the electricity system at all time steps to ensure that essential grid supporting services such as frequency control or voltage support are available in the system at all times. This allows *medea* to approximate real operating conditions of an electricity grid and to qualify its results as a base for realistic recommendations on policies to design a functioning electricity system in the future. Further details and a mathematical description of *medea* can be found in Wehrle et al. (2021).

For the purpose of this study, *medea* was amended in several aspects compared to the study by Wehrle et al. (2021). First, H_2 was included as an additional energy carrier that can be produced and stored endogenously in the system to meet the exogenously defined H_2 demand. Second, an import option was implemented that allows *medea* to obtain H_2 from outside the model for a fixed price. To prevent unrealistic peaks in H_2 imports that might occur from the attempt of the optimization algorithm to minimize H_2 storage costs, hourly H_2 import capacity was fixed to a 1/8760 part of annual H_2 imports, which were endogenously determined by *medea*. Third, the equations governing the content of energy storage units were changed so that *medea* could endogenously and freely determine the ideal storage content at the beginning of the simulation. This prevents that externally determined initial storage capacity and content affect the simulation results. To avoid an energy imbalance in the simulation, the storage content of the first hour of the simulation was fixed to match the storage content of the last hour of the simulation. Fourth, hot water tanks were added as a possible technology to store heat energy to introduce the possibility of a flexible heat production through heat pumps at times where intermittent electricity is abundant. Fifth, energy losses over time were implemented for battery and heat energy storage units as such time losses considerably affect their efficiency for long-term energy storage. Sixth, ancillary services were optimized so that the same unit of a technology could not feed and draw electricity from the grid at the same time,

which was important to realistically represent ancillary services by electricity storage units in the model.

4.2 Modelling Approach

In order to account for short-term and long-term variations in intermittent renewable generation, the model was simulated with a 1-hour time resolution over the course of a full year to capture intra-daily and seasonal dynamics of intermittent electricity generation. The year 2040 was chosen as a reference year for this study as it represents a time where AT intends to achieve climate neutrality (Österreichischer Nationalrat, 2021) and when DE wants to have largely decarbonized its energy sector (Deutscher Bundestag, 2022a). Therefore, it can be assumed that "hard-to-decarbonize" sectors such as the steel industry represent some of the last sectors that need to be decarbonized in 2040. This is in line with the goal to compare the effects of a direct and indirect electrification of *iron making* on "mature" renewable electricity systems. Even though it is uncertain to what extent the Austro-German I & S industry can actually be decarbonized in 2040 due to the long investment cycles and the current immaturity of near-zero *iron making* technologies (IEA, 2020), this study thereby represents a what-if analysis that explores the impacts of an ambitious decarbonization of the Austro-German I & S industry.

For the simulation, *medea* was allowed to use all already installed renewable technologies in AT and DE and further renewable technologies, which ensure that all considered energy carriers (electricity, heat and H_2) could be produced by at least three different technologies and stored in at least one type of storage unit. Altogether, *medea* could use 20 different energy generation or storage technologies as well as H_2 imports to meet exogenous energy demands. Figure 6 summarizes the energy carriers that were considered in this study and indicates the resulting possible connections between energy carriers in the modelled system.

To ensure that *medea* simulates electricity systems that also resemble the politically declared grid expansion goals in AT and DE, *medea* was fed with initial input capacities that represent technology-specific political expansion targets in AT and DE. Accordingly, this study did not pursue a greenfield modelling approach. Table 1 indicates the initial capacities that were used as an input for the model and which are further described in the Section 4.3.1. They are relevant to the model approach as initial capacities do not induce investment costs but only add costs from operations and maintenance (O & M) and fuel (imports) to the system costs. The system costs, therefore, do not represent the overall system costs for building and maintaining a 100 % renewable electricity system in AT and DE from scratch but represent the additional system costs from expanding the given system.

To prevent an unrealistic expansion of installed capacities during the simulation, the actual use of some technologies was limited to a maximum capacity according to given technical or geographical constraints. First, *ror* capacities could not be expanded beyond the initially installed capacities as it is unlikely that more *ror* power plants can be realized beyond the already ambitious expansion target in AT (+5 TWh generation from *ror* in 2030) and beyond an estimated *ror* potential in DE (see Section 4.3.1). Second, hydro storage capacities were fixed to the initially defined storage capacities as both pumped hydro and hydro reservoir storage have large area requirements, which will very likely impede a considerable expansion of hydro storage technologies. Third, electricity production from biomass was capped as the overall amount of biomass that can be sustainably used is limited by the available agricultural and forest areas. Furthermore, using biomass for electricity generation reduces the biomass that is available as a renewable resource in other sectors such as the construction sector. In AT biomass power plants were limited to 6.7 TWh/year as this represents the maximum estimated electricity production from biomass according to Krutzler et al. (2016) and far exceeds the 4.4 TWh electricity generated from biomass in 2021 (E-Control, 2022). In DE, biomass power plants were limited to 56 TWh electricity output per year, which represents electricity generation from biomass in 2020 (Umweltbundesamt, 2022) plus a margin of 10 % to account for a possible increase in electricity generation from biomass in the future. Fourth, hourly H_2 imports were capped to a 1/8760th of annual H_2 imports to simulate an H_2 import capacity imposed by the available technical H_2 import infrastructure (pipelines or ship terminals). This prevents

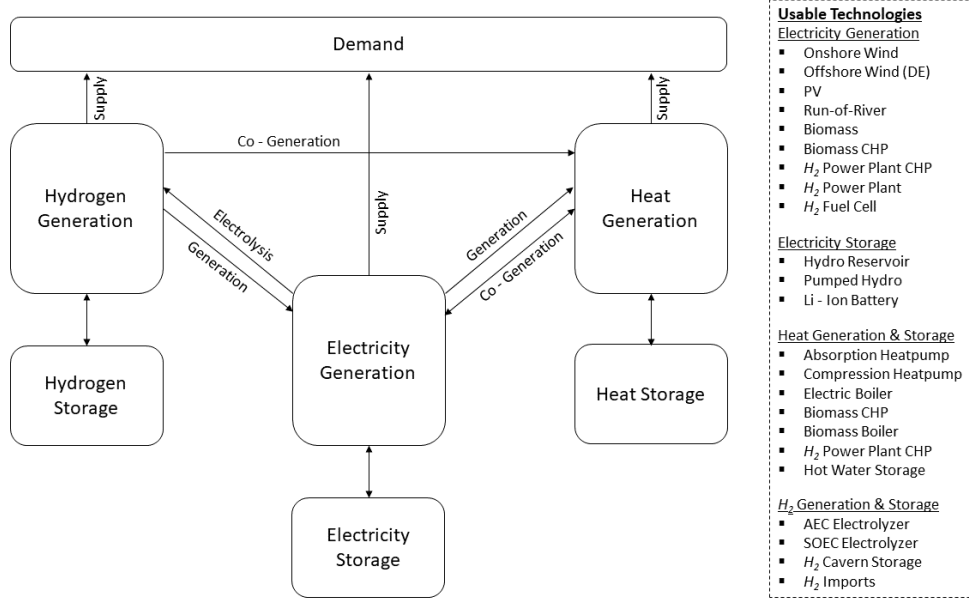


Figure 6: Schematic representation of the modelled system. Several different generation and storage technologies could be used in the model in order to meet the fixed external demand for electricity, heat and H_2 . As various technologies allow a conversion or co-generation between the energy carriers, the used model represents a highly coupled energy system.

unrealistic H_2 import peaks to satisfy H_2 demand when domestic H_2 generation is low. A cap on hourly H_2 imports, therefore prevents that H_2 storage capacities are underestimated. Fifth, the offshore wind capacity in DE was capped to 70 GW to account for zones along the German coast that cannot be used for offshore wind parks, for example to preserve environmental protection areas. Lastly, the electricity exchange capacity between AT and DE was set to 5.4 GW (Wehrle et al., 2021) to prevent extreme electricity imports or exports in AT that could incentivize the model to install wind or PV capacities only in the region with the respectively better production conditions.

To systematically investigate the behaviour of the Austro-German energy system under different constraints as defined through the research questions, this study calculated a total of 42 scenarios, in which energy demand and supply were modelled hourly in both AT and DE. From these 42 scenarios, half of the scenarios assumed that *iron making* was completely based on H_2 DR (" H_2 scenarios") and the other half that *iron making* was based on iron ore electrolysis (" el scenarios"). The H_2 and el scenarios, therefore, only differed in their hourly and overall electricity and H_2 demands as will be discussed in Chapter 4.3.3. For each *iron making* technology, the following possible capacity constraints were assumed in different scenario groups: (1) no constraints; (2) wind constraint: onshore wind capacities in AT and DE were limited to the initial capacities and could not be expanded; and (3) wind and PV constraint: onshore wind and PV capacities could both not exceed the initial defined capacities. For each combination of el/H_2 scenario and capacity expansion constraint, one scenario was calculated that assumed a different H_2 import price with seven H_2 prices ranging from 30 €/MWh H_2 to 90 €/MWh H_2 in 10 € steps. All data were prepared with Python 3.9.7, while model constraints and the model were formulated in GAMS 38.2.1. The code used for this project is available on the GitHub repository [simobu/medea_decarbonizing_steel_industry](https://github.com/simobu/medea_decarbonizing_steel_industry) (Büttner, 2023).

Since *medea* provides a wide range of data on the modelled system, this study focused on selected model variables to answer the above mentioned research questions. Firstly, data on system costs were analyzed by country and cost type (e.g. investment cost, fuel costs, O & M,...) to identify the main economic differences between the economically ideal electricity systems in the modelled scenarios. Secondly, the scenarios were analyzed according to their gross electricity

consumption (GCE), which represents the electricity that is originally needed to meet the energy consumption in each country. This was calculated for each country by subtracting electricity exports (and vice versa adding electricity imports) from gross electricity generation and by adding the electricity entailed in H_2 imports (assuming a conversion efficiency of 71.5 %). GCE, therefore, combined both the electricity that is directly and indirectly consumed in a country, regardless of where the electricity was generated, and thereby allows to compare the energy consumption of scenarios with different shares of direct and indirect electrification.⁴ Thirdly, H_2 production and import data were further analyzed to evaluate the relevance of domestic green H_2 production in 100 % renewable electricity systems in AT and DE.

4.3 Data

The following section describes the input data that was used to parameterize the model used in this study.

4.3.1 Initial Capacities

In DE, PV, onshore wind, and electricity generation capacities from biomass were taken from §4 of the Renewable Energy Act 2023 (Deutscher Bundestag, 2022a). Similarly, the initial H_2 cavern storage output capacity and H_2 gas power plant capacities were derived from the goals for " H_2 -based electricity storage" (§28f) and for "electricity generation from green H_2 " (§28g). The initial offshore wind capacity of 55 GW represents the average of the 40 GW (2035) and 70 GW (2045) expansion goals defined in the German "Wind-at-sea-law" (Deutscher Bundestag, 2022b). For run-of-river (*ror*) power plants, the initial 6.2 GW capacity was derived from the maximum realizable *ror* potential in DE described in Keuneke (2019). All initial output and energy storage capacities for biomass combined heat and power (CHP) plants and hydro storage technologies in DE and AT were taken from Wehrle et al. (2021).

In AT, the target capacities for onshore wind, PV, and *ror* were calculated based on the electricity generation goals as defined in the Austrian "Renewable Expansion Act" (Österreichischer Nationalrat, 2021). Since the Renewable Expansion Act only defines targets for additional energy generation compared to 2020, these energy targets were converted into generation capacities based on the assumed full-load hours of onshore wind, PV and *ror* in AT as provided by Wehrle et al. (2021). Subsequently, these estimated additional capacities were added to the installed capacities in 2020 provided by ENTSO-E (n.d.) (onshore wind and *ror*) and by Biermayr et al. (2022) (PV). Biomass capacities were adopted from Wehrle et al. (2021). In both AT and DE, the initial electrolyzer capacities were taken from the respective national H_2 strategies (BMK, 2022; BMWK, 2020). In both countries, the initial capacities for all other technologies were set to zero.

4.3.2 Base Energy Demands

Hourly electricity demands for 2040 in AT and DE were taken from the electricity load time series of the climatic year 2009 in the Distributed Energy Scenario in the ten-year network development plan (TYNDP) published by ENTSO-E (2022). The dataset includes electricity demands from residential, industrial and tertiary consumers and already considers an advanced electrification of the transport and heat sectors. It explicitly includes additional energy demands from electric vehicles and from domestic and district heating (DH) heat pumps (HPs). As DH represents an essential part of *medea*, the annual electricity demand from DH HPs was

⁴GEC differs from the exogenous gross electricity demand as it includes the endogenous energy demand as well as the energy losses during energy conversions, which were both determined by *medea*. Differences in GEC can therefore, be considered as variations in the energy efficiency between scenarios. Since exogenous energy demand was in this study assumed to be slightly higher in H_2 scenarios than in *el* scenarios, H_2 scenarios should exhibit a slightly higher GEC if the respective energy systems had the same overall energy efficiency. Please note that heat production from biomass as well as H_2 transport losses (e.g. during liquefaction or conversion to ammonia) are not included into GEC in this study. Therefore, GEC does not represent the gross energy consumption of the entire energy system modelled in this study.

Table 1: Initial capacities that were used as an input into the model.

	AT	DE
unit	GW	GW
PV	12.4	400
Run-of-river	6.8	6.2
Wind Onshore	7.1	160
Wind Offshore	-	55
Biomass	0.7	4.2
Biomass CHP	0.4	4.2
Biomass Boiler	0.8	2.6
Heatpump Compression	0	0
Heatpump Absorption	0	0
Electric Boiler	0	0
Battery (Li-Ion)	0	0
Hydro - Reservoir Storage	3.5	0.2
Hydro - Pumped Storage	5.2	7
SOEC Electrolyzer	0	0
AEC Electrolyzer	1	10
H2 - Cavern Storage	0	4.4
Fuel Cell	0	0
H2 Power Plant	0	4.4
H2 CHP Power Plant	0	0
Hot Water Tank	0	0

subtracted from the overall electricity demand in the TYNDP to prevent a double counting of DH energy demands. As a result, annual electricity consumption in AT was 105.1 TWh and 809.4 TWh in DE.

Similarly, annual H_2 demands from the industry and transportation sectors in AT and DE were also taken from the Distributed Energy Scenario in the TYNDP 2022 (ENTSO-E & ENTSOG, 2022). Since the TYNDP does not provide hourly H_2 load data, the H_2 demand was assumed to be perfectly flat. Altogether, annual H_2 demand was 17 TWh H_2 (1.94 GW H_2) in AT and 251.2 TWh H_2 (28.67 GW H_2) in DE. H_2 demands from the residential and tertiary sectors were not considered in this study.

The annual DH heat demand in DE was taken from Prognos, Öko-Institut and Wuppertal Institut (2021), which estimate that 158 TWh of heat energy must be provided to district heating networks in 2040. For AT, Baumann, Martin and Pauritsch, Günter and Rohrer, Michael and Schweitzer, Marcel (2022) estimate that about 31.4 TWh heat energy must be provided to DH networks in AT in 2040. As this study did not model all DH technologies that will likely provide heat energy to DH networks such as geothermal heat power plants or industrial waste heat, only 75 % of the above-mentioned DH demands entered *medea* as heat input demand. These heat energy demands of 23.6 TWh in AT and 118.5 TWh in DE were subsequently translated into hourly heat energy demand time series based on 2018 daily average temperature and standard NG load profiles as described in Wehrle et al. (2021).

4.3.3 Energy Demand from *Iron Making*

To accurately represent energy demands from different *iron making* processes, scenario specific hourly electricity and H_2 demands from *iron making* were added to the respective demand time series described above. As I & S production facilities typically seek to maximize plant utilization rates (Pimm et al., 2021), electricity and H_2 demand from steel production were added as a perfectly flat time series, which assumes that all steel production facilities run all year around at the same capacity. In a first step, specific energy demands for *iron making* were

derived as average values from selected literature values on the expected energy consumption for H_2 -based DR and EW/MOE. Table 3 provides a summary of the expected energy consumption from H2DR and EW/MOE and the range found in the literature. It indicates that electricity-based *iron making* is expected to be more energy efficient than H_2 - based *iron making*. Either way, H_2 or electricity-based *iron making* are expected to consume less energy than a typical BF (3.68 MWh/t steel according to Vogl et al. (2018)). The energy demands in Table 3 represent energy demands solely for the *iron making* process and do not include energy consumption from other processes involved in near-zero carbon steel production such as energy consumption from EAFs. Electricity demand from EAFs was explicitly not considered in this study as it remains constant across all scenarios in this study and is already partially included in the TYNDP electricity demand (see scenario assumption of the TYNDP in ENTSO-E and ENTSG (2022)).

Total hourly energy demands for *iron making* were then estimated using technology specific *iron making* energy demands and the average steel production quantity in AT and DE over the past five years (Table 3). The calculation further assumed that primary steel production represents 50 % of overall steel production with the other half of steel production originating from secondary steel production. This translates into an annual reduced Fe demand of 3.71 Mt in AT and 20.11 Mt in DE. Multiplied with technology specific *iron making* demands, H2DR therefore increased hourly H_2 consumption by 0.83 GW and hourly electricity load by 0.25 GW in AT while electricity-based *iron making* raised the hourly electricity load by 1.27 GW. In Germany, H_2 -based steel production constantly required 1.37 GW of electricity and 4.51 GW H_2 while iron oxide electrolysis technology increased electricity load by 6.89 GW.

Table 2: Crude Steel Production 2017 - 2021 in AT and DE in millions tons per year. From: World Steel Association (2022)

Year	AT	DE
2017	8.14	43.30
2018	6.89	42.44
2019	7.42	49.63
2020	6.77	35.68
2021	7.88	40.01
average	7.42	40.22

Table 3: Energy demands to produce one ton of reduced Fe through iron oxide electrolysis or H2DR. Values assumed in this study represent averages of the considered literature values. Note that it requires 1.40 MWh electricity to produce 1 MWh H_2 at an electrolyzer efficiency of 71.5 %

Technology	Energy Carrier	This Study	Range in Literature	Literature
		MWh	MWh	
H2DR	Electricity	0.60	0.60	[1]
	H_2	1.97	1.7 - 2.35	[1] - [7]
Electrolysis	Electricity	3.00	2.72 - 3.50	[3], [8] - [12]

Literature: [1] Bhaskar et al. (2020), [2] Bailera et al. (2021), [3] Fan and Friedmann (2021), [4] Venkataraman et al. (2022), [5] Vogl et al. (2018), [6] Mayer et al. (2019), [7] Victoria et al. (2022), [8] Cavaliere (2019), [9] West (2020), [10] Lechtenböhmer et al. (2016), [11] Allamore et al. (2010), [12] Barberousse et al. (2020)

4.3.4 Costs and Prices

Table 4 shows the assumed costs for investments and operation and maintenance (O & M) of the technologies considered in this study as well as the assumed lifetime. Technology specific lifetimes were used to calculate investment and O & M cost annuities at a discount rate of 5 %. For PV, it was assumed that free field PV parks and roof mounted system provide equal shares of all considered capacities. All price data were converted to 2020 € using the producer price index (total market) for the Euro area from OECD (2022).

5 Results

5.1 System Costs

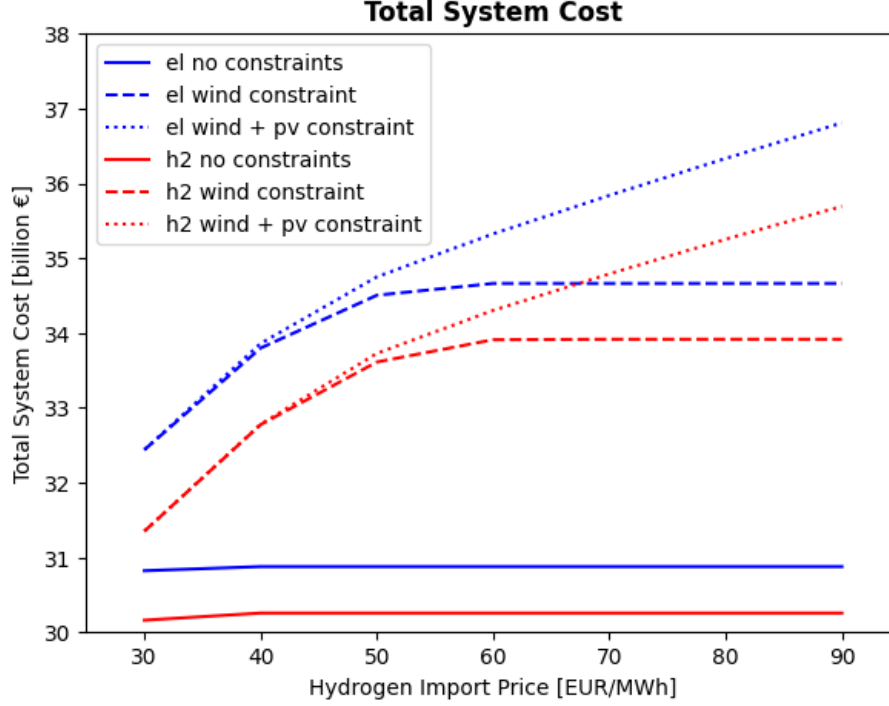


Figure 7: Total annual energy system costs of all modelled scenarios. Note: the costs shown in this plot do not entail all costs associated with the modelled energy systems. For example, investment costs for initially installed generation capacities or costs for the internal electricity grid were not included in the cost optimization of *medea*. Therefore, the system cost values cannot be taken as the real annualized costs of the respective energy system.

Figure 7 shows the annualized system costs of all 42 energy systems modelled in this study. As can be seen, the system costs vary considerably between scenarios and across different hydrogen import prices. First, system costs of all scenarios with electricity-based *iron making* (*el scenarios*, blue lines) were always higher than system costs in scenarios with H₂DR-based *iron making* (*H₂ scenarios*, red lines). Second, total system costs rose considerably as constraints were imposed on the maximum installed onshore wind and PV capacities. At a H₂ import price of 90 €/MWh, limiting onshore wind capacities to the announced capacity goals increased annual system costs by 12.1 - 12.3 % while an additional limit on PV capacities increased total system costs by 18.0 - 19.2 % compared to the no constraint scenarios. Third, H₂ import prices did not affect system costs above 40 €/MWh in the no constraint scenarios and not above 60 €/MWh in the wind constraint scenarios. In scenarios with wind and PV constraints, higher H₂ import costs increased system costs across all considered H₂ prices.

To understand why system costs differed between *el* and *H₂* scenarios, system costs were further disaggregated into individual cost components in Figure 8. It displays the cost differences of various cost components (colored bars) between *el* and *H₂* scenarios as well as the overall system cost differences between the respective *el* and *H₂* scenarios (black lines). All *el scenarios* were characterized by higher costs from (1) investments into new generation capacities (blue), (2) from O & M costs for the installed capacities (orange), and (3) from investments into additional energy storage capacities (grey). Fuel costs for biomass (green), on the other

hand, did not strongly differ between *el* and H_2 scenarios except in constraint scenarios at a H_2 import price of 50 €/MWh. In these cases, *el* scenarios used considerably more biomass for energy generation than H_2 scenarios. Surprisingly, H_2 scenarios did not consistently import more H_2 than *el* scenarios as the cost difference for H_2 imports shows. In contrast, *el* scenarios imported more H_2 than the respective H_2 scenarios in most wind and PV capacity constraint scenarios.

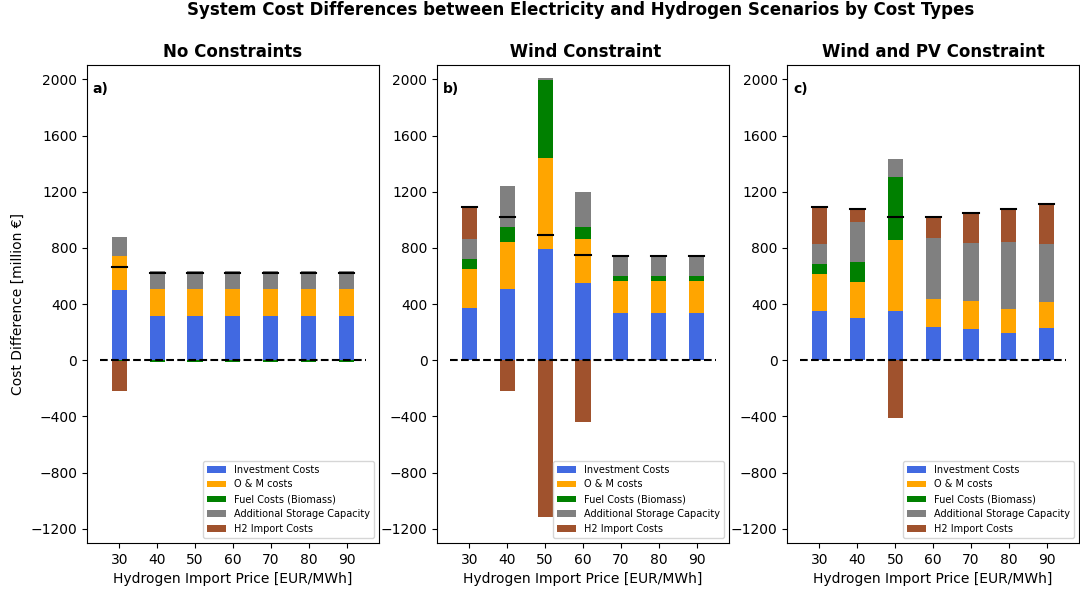


Figure 8: System cost differences disaggregated into five cost types. The bars show the difference between the respective costs in the *el* scenario and the related H_2 scenario. Positive values indicate higher costs in the *el* scenario while negative values represent higher costs in the respective H_2 scenario. The black bar indicates the sum of the cost differences between the H_2 and *el* scenarios. Note that the shown values do not represent the total costs from a cost type and are also not representative for the relative costs of each cost type to the total system costs. I.e. the absence of a bar for "Fuel Costs (Biomass)" simply indicates that the fuel costs for biomass are identical in both scenarios even though they might actually represent a considerable share of the total system costs.

Since investment costs into new generation capacities and the associated O & M costs represented a major cost differences between *el* and H_2 scenarios, investment cost differences were further analyzed in Figure 9. It displays the investment cost differences between *el* and H_2 scenarios by technology and shows that *el* scenarios consistently invested into larger H_2 gas power plant capacities than H_2 scenarios, which in turn consistently invested more into electrolyzer capacities. The investments into H_2 gas power plants thereby constituted the largest investment cost difference between *el* and H_2 scenarios in almost all considered cases. *El* scenarios also almost consistently required larger electricity storage output capacities except under high H_2 import prices in the wind and PV constraint scenarios. Like in Figure 8, *el* scenarios invested exceptionally more into biomass capacities at a H_2 import price of 50 €/MWh in the constraint scenarios, which indicates a pronounced difference between *el* and H_2 scenarios at this H_2 import price. Interestingly, investments into wind or PV capacities differed only in a few scenarios and did not represented a major investment cost difference between *el* and H_2 scenarios.

Looking at the electricity system of each country individually (see Figure A.1) revealed marked differences between AT and DE. In DE, system costs were very similar to overall system costs, which is not surprising as the German electricity system contributed 85 - 92 % of the overall system costs in all scenarios. Like in the overall system, *el* scenarios were in

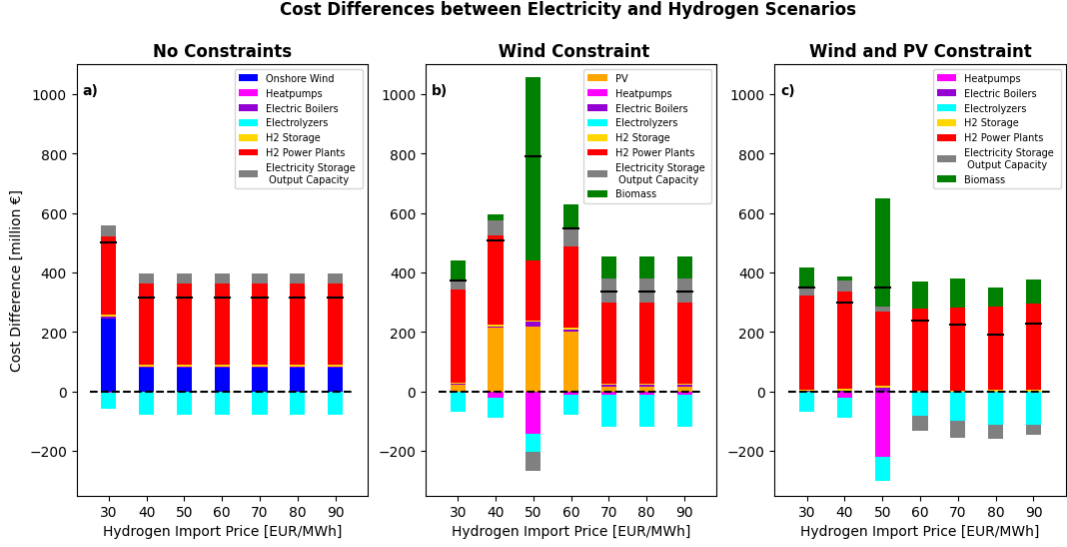


Figure 9: Investment cost differences by technologies. The bars show the difference between the respective costs in the *el scenario* and the related H_2 *scenario*. Positive values indicate higher costs in the *el scenario* while negative values represent higher costs in the respective H_2 *scenario*. The black bar indicates the sum of the investment cost differences between the H_2 and *el scenarios*. Note that the shown values do not represent the total investment costs per technology and are also not representative for the relative costs of each technology to the total system costs. I.e. the absence of a bar for "Wind onshore" simply indicates that the investment costs for onshore wind power plants are identical in both scenarios even though they might actually represent a considerable share of the total system costs.

all cases more expensive than H_2 *scenarios* in DE as the German electricity system required relatively more flexible electricity generation technologies in the *el scenarios*, primarily in the form of expensive H_2 gas power plants. In the wind constraint scenarios, however, system costs in both AT and DE showed an unexpected behavior. While system costs almost doubled in AT in the wind constraint scenarios as H_2 import prices rose above 40 €/MWh, system costs in DE decreased as H_2 import prices increased from 40 to 60 €/MWh. While such a cost distribution might optimize overall system costs, it indicates that AT built overproportionally more energy infrastructure in these scenarios, which would have been installed in DE when both countries would have been analyzed individually. And indeed, the wind constraint scenarios showed an extreme peak in installed PV and battery storage capacities in AT with almost 7 times (72.5 GW) more PV capacity installed than declared in the expansion target goals and almost 10 times (50.5 GWh) more battery storage capacity installed than in the wind and PV constraint scenarios. Consequently, the wind constraint scenarios represent outlier scenarios and should be interpreted with care.

In contrast to DE, flexible electricity generation capacities such as H_2 power plants or battery storages were not an important distinguishing factor between *el* and H_2 *scenarios* in AT (Figure A.2). Conversely, H_2 imports were the main factor that distinguished *el scenarios* from H_2 *scenarios* in the Austrian electricity system. As H_2 *scenarios* consistently imported more H_2 than the respective *el scenarios*, the Austrian electricity system showed a very different behavior than the German electricity system. In particular, the wind and PV constraint scenarios show considerably increased system costs from H_2 imports in the **\$H_2\$ scenarios**. Investment and O & M costs, on the other hand, only differed between *el* and H_2 *scenarios* in the wind constraint scenarios where exceptionally large PV capacities were installed in AT. As described above, these scenarios represent outlier scenarios and cannot be seen as a reliable representation of a realistic electricity system in AT.

In summary, electricity-based *iron making* did not decrease the overall system costs compared to H_2 -based *iron making* as expected by hypothesis 1. In contrast, electricity-based *iron making* even increased overall system costs as more expensive flexible electricity generation capacities were required in DE to bridge the gap between a iron oxide electrolysis induced higher direct electricity demand and intermittent electricity generation. H_2 fired gas power plants thereby represented the largest individual cost component that distinguished *el* and H_2 scenarios. This effect could, however, only be observed in the German electricity system, which strongly affected the results of the overall system due to its relative size compared to the Austrian electricity system. In AT, electricity-based *iron making* reduced the electricity system costs at least in the wind and PV constraint scenarios. In these scenarios, H_2 imports increased the costs for the H_2 scenarios as AT did practically not produce H_2 on its own. In scenarios where wind and PV capacities could be expanded without restrictions, the costs of the Austrian electricity system did not significantly differ between *el* and H_2 scenarios.

5.2 Gross Electricity Consumption

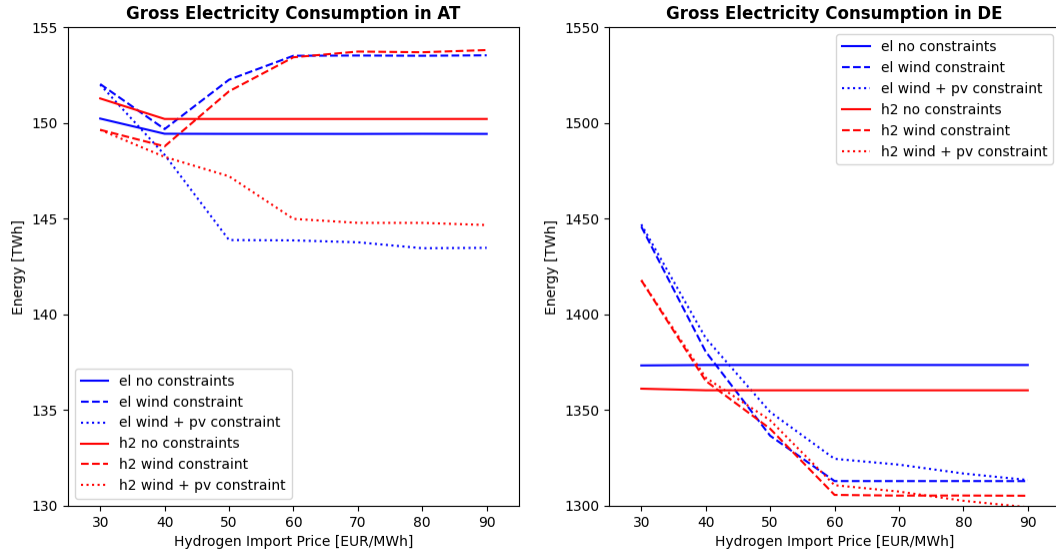


Figure 10: Gross electricity consumption in AT and DE. This metric includes all electricity that is directly or indirectly consumed in each country regardless of where the electricity was produced. In particular, it includes the electricity that was necessary to produce the green H_2 that is consumed in each country.

Figure 10 shows the GEC of all scenarios in AT and DE.

In DE, the GEC shows (1) that *el* scenarios consistently consumed more electricity than H_2 scenarios despite their lower exogenous energy demand and (2) that gross electricity consumption strongly increased in scenarios with capacity constraints below H_2 import prices of 60 €/MWh. Both phenomena were closely connected to electricity production from H_2 gas power plants (Figure 11) as H_2 gas power plants produced between 17.7 - 61.0 TWh of electricity in all scenarios in DE. Furthermore, *el* scenarios always required more electricity from H_2 power plants than the corresponding H_2 scenarios. Considering that electricity generation from green H_2 has a very low efficiency⁵, producing the above mentioned quantities of electricity from H_2 gas power plants resulted in energy losses of 22.2 - 76.6 TWh electricity that needed to be additionally produced to supply the same final electricity demand. Compared to the H_2 scenarios, producing electricity from green H_2 still resulted in higher energy losses in

⁵this study assumes 44.3 %, excluding energy losses during H_2 storage or transport

the *el scenarios* as converting H_2 into electricity involves higher losses than the gross energy difference between H_2 -based *iron making* and electricity-based *iron making*. Figures 10 and 11 show that the additional losses from H_2 -based electricity generation in the *el scenarios* were able to offset the gross energy efficiency gains from electrolysis-based *iron making*. Besides high energy losses from inefficient H_2 power plants, the energy efficiency of the *el scenarios* was further undermined by additional energy losses in electricity storages. Similarly, falling H_2 prices incentivized the use of inefficient H_2 power plants, which explains the increasing GEC below 60 €/MWh H_2 in scenarios with capacity constraints. This raise of GEC at low H_2 prices was further enhanced by a substitution of biomass-based heat generation, which does not count into GEC, with electricity-based heating technologies, which counts into GEC.

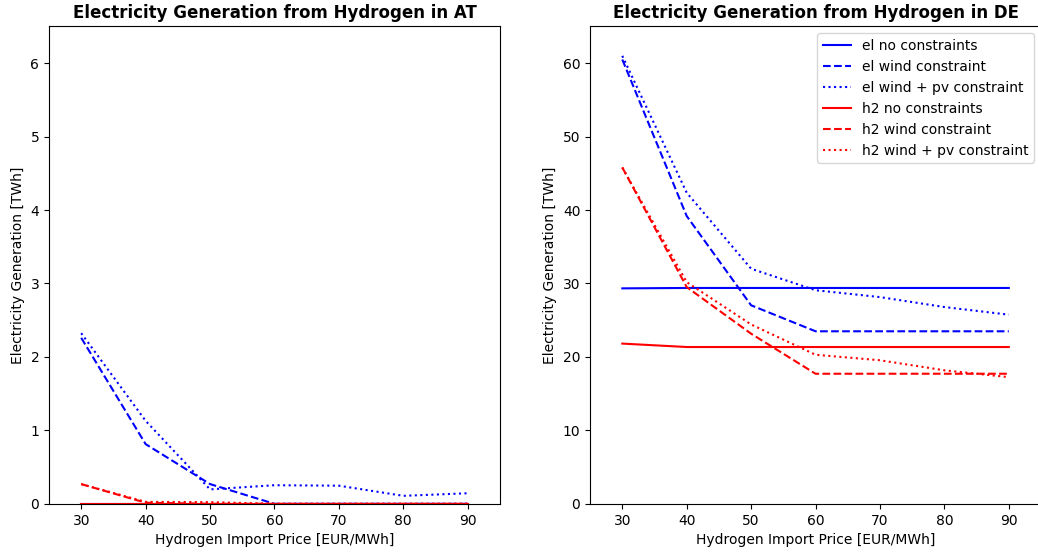


Figure 11: Electricity generation from H_2 gas power plants in AT and DE. While H_2 gas power plants were present in all scenarios in DE, they were only sparsely used in a few scenario in AT.

In AT, GEC strongly differed between scenarios with different constraint assumptions. The main differences between these scenario groups were: (1) dissimilar DH technologies, (2) varying energy losses in storage units, and (3) different levels of electricity curtailment. In contrast to DE, H_2 -based electricity generation (see Figure 11) did considerably affect GEC in AT except in a few *el scenarios* at low H_2 import prices. Above 60 €/MWh, wind constraint scenarios consumed almost 10 TWh (about 7 %) more electricity than scenarios with wind and PV capacity constraints, while no constraint scenarios had an intermediate GEC. The wind and PV constraint scenarios were characterized by a low GEC primarily due to a substitution of about 5.4 TWh electricity with biomass for DH compared to the no constraint scenarios. Since biomass-based DH did not count into GEC, this decreased GEC. The high GEC observed in the wind constraint scenarios, on the other hand, resulted from a mix of additional energy losses in batteries (+ 2.6 - 3.1 TWh compared to no constraint scenarios) that were required to buffer the extraordinarily large PV generation capacities and additionally from increased curtailment of energy (+ 2.6 - 2.7 TWh compared to no constraint scenarios). Even though these energy losses were partly compensated by a more electrified DH sector (+ 1.7 - 2.0 TWh), GEC in wind constraint scenarios still was about 3.6 - 4.0 TWh higher than in the no constraint scenarios. As described above, the wind constraint scenarios must however be interpreted with care. All differences between scenarios largely vanished at very low H_2 import prices so that AT consumed between 149.6 - 152.0 TWh of gross electricity.

5.3 H_2 Production and Imports

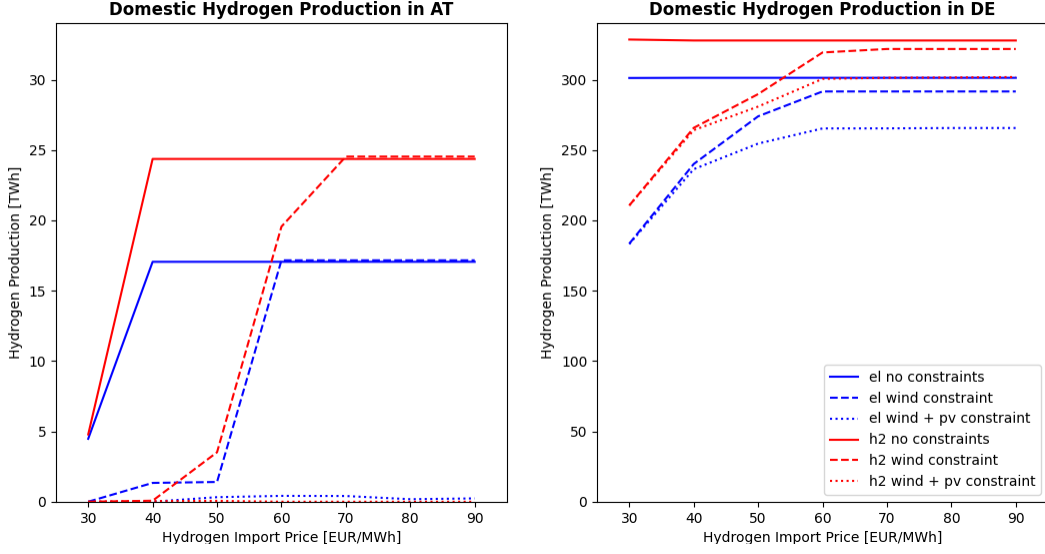


Figure 12: Annual domestic H_2 production in AT and DE by H_2 import prices in all considered scenarios. While DE produced more than 183 TWh H_2 in all scenarios, AT did in some scenarios not produce any H_2 .

Figure 12 shows the annual H_2 production in AT and DE. While at least 183 TWh H_2 were produced in the German electricity system in all scenarios, AT produced only considerable quantities of H_2 in the wind constraint and no constraint scenarios. Fittingly, H_2 imports into AT and DE were low in scenarios with a high domestic H_2 production (Figure A.6). In particular, both AT and DE did not import any H_2 in no constraint scenarios above 30 €/MWh H_2 and in wind constraint scenarios not above 70 €/MWh H_2 . Consequently, AT and DE were completely self-sufficient in their electricity and green H_2 supply in these scenarios. Interestingly, domestic H_2 production exceeded H_2 imports in all scenarios in DE, indicating that domestic H_2 production was economically feasible in DE. And indeed, electrolyzers achieved more than 4000 full load hours⁶ (FLH) in all scenarios in DE and more than 4500 FLH in 33 out of 42 scenarios. In contrast, Austrian electrolyzers reached a much wider range of FLH from below 1000 to more than 7800 FLH. This indicates that electrolyzers were used as regular part-time electricity consumers in all scenarios in DE, whereas they were used very differently in AT. In particular, all scenarios in DE showed a distinct H_2 production pattern over the course of one day with a peak in H_2 production around noon and with lower production during night hours (7 pm to 6 am, Figure refA.7). In contrast, only the wind constraint scenarios with exceptionally high PV capacities displayed a similar pattern in H_2 production in AT. In all other scenarios, Austrian electrolyzers produced H_2 with almost flat profiles over the course of an average day. Over the course of a year, no distinct seasonal H_2 production patterns were recognizable in either country.

H_2 import data further show that 60 €/MWh marked a threshold below which imports into the 100 % renewable Austro-German electricity system became increasingly competitive. While H_2 imports were only competitive with domestic H_2 production in a few scenarios at 90 €/MWh, H_2 imports were strongly expanded below 60 €/MWh in all scenarios with capacity constraints in both AT and DE. In these scenarios, H_2 imports distinctively differed between *el* and H_2 scenarios at 50 €/MWh H_2 indicating that H_2 scenarios could import more H_2 in an economically viable way than *el* scenarios. Due to these higher H_2 imports, H_2 scenarios required relatively less electricity for domestic H_2 production while at the same time relatively

⁶Full load hours describe how much a technology is used over the course of a year. They are calculated by dividing the annual output by the number of hours in a year (8,760)

more H_2 could be used for flexible electricity generation. In sum, both effects strongly reduced the overall demand for electricity generation from biomass (- 13.5 TWh electricity generation from biomass in DE in wind constraint scenario) as was already noted above.

6 Discussion

This study shows that different approaches to decarbonize the steel industry can considerably influence the set-up of the electricity systems in AT and DE. In particular, the findings highlight that measures to decarbonize steel production through H_2 or electricity should be analyzed not only by their individual energetic and economical performance but also by their effects on the underlying electricity system. Even though iron ore electrolysis was expected to increase the gross energy efficiency of the energy system (hypothesis 2), the results show that electricity-based *iron making* can actually decrease overall energy efficiency as was observed in this study. Furthermore, electricity-based *iron making* also translated into 2.1 - 3.5 % higher annual costs for the Austro-German electricity system. Accordingly, decarbonizing steel production considerably affects the electricity system of AT and DE and should therefore be carefully considered in future plans to decarbonize the I & S industry.

6.1 Differences between AT and DE

The results of this study further show that a decarbonized steel production differently affected completely renewable electricity systems in DE and AT. While electricity-based *iron making* increased the costs and GEC of the German electricity system in all scenarios, it reduced costs and GEC in most scenarios in AT. The main difference between the Austrian and German electricity systems could be observed in the required capacities of flexible storage and electricity generation units. While in AT only little new electricity storage capacities had to be added in the form of batteries, the German electricity system required large new battery and H_2 gas power plant capacities to obtain a well-functioning renewable electricity system. Furthermore, electrolyzers appeared to play an important role as flexible electricity consumers in the German electricity system. In AT, electrolyzers were on the other hand no relevant flexible electricity consumers.

The results for the Austrian electricity system can be explained by its large existing hydro storage capacities (3.279 GWh), which are capable of long-term electricity storage and can therefore provide high flexibility to the Austrian electricity system. Even though the Austrian electricity system also required between 1.1 and 13.6 GWh⁷ of battery storage capacity, it required little to no expensive H_2 gas power plants at H_2 prices above 60 €/MWh. Since H_2 gas power plants were the main driver of additional system costs in the *el scenarios*, *el scenarios* did therefore not increase system costs in AT compared to the respective H_2 scenarios except in a few outlier scenarios. In fact, the existing long-term storage capacities were sufficient to buffer variations in electricity generation and demand over longer time periods. Furthermore, they were also able to bridge the higher gaps between electricity generation and demand even when electricity demand was elevated from electricity-based *iron making*.

The German electricity system, on the other side, required large battery storage and H_2 gas power plant capacities in all scenarios as only little renewable storage capacities are currently installed in DE. With only about 238 GWh of hydro storage capacity, the current German electricity system is not able to cope with the large differences between intermittent electricity generation and electricity consumption in a completely renewable system. As expanding hydro storage capacities was assumed to be infeasible, additional long-term electricity storage could only be realized through an intermediate storage of electricity as H_2 , which could be reconverted to electricity in H_2 gas power plants. Accordingly, H_2 gas power plants were in DE essentially required to replace the missing long-term electricity storage capacities in the system. This also holds for H_2 that was imported into DE and subsequently used in H_2 power plants as importing

⁷Excluding outlier wind constraint scenarios, where battery storage capacities climb to 56.3 GWh

green H_2 essentially represents indirect electricity imports. Besides long-term storage capacity, large battery storage capacities were required in the German electricity system in all scenarios.

Interestingly, these additional storage capacities were the most important drivers of electricity system costs in DE. As Figures 8 and 9 show, additional storage capacity and additional H_2 gas power plants represented in most cases the largest extra cost in the *el scenarios*. Even though H_2 power plants produced only little extra electricity, they nevertheless increased system costs noticeably. In the wind and PV constraint scenario at 90 €/MWh for example, H_2 gas power plants in DE produced only 8.5 TWh more electricity than in the respective H_2 scenario. While this might appear small compared to the 1309.6 TWh of electricity generated⁸ in DE in this scenario, these additional 8.5 TWh (0.6 % of annual electricity generation) raised annual system costs by 1.29 billion € (plus 3.6 % compared to the overall system costs in the H_2 scenario) only through investments into H_2 gas power plants, higher O & M costs for H_2 power plants and additional H_2 imports. This corresponded to additional costs of 151.76 € for every additional MWh electricity that was generated from H_2 .

6.2 The Role of Flexibility in DE

While H_2 gas power plants and battery storages added considerable flexibility to balance electricity generation and demand in the German electricity system, electrolyzers were another main source of flexibility in DE. To evaluate the relevance of flexible electricity generation and flexible electricity consumption, Figure 13 displays (1) the share of electricity that was fed into the grid by flexible generation units (electricity storage units, biomass power plants, H_2 power plants) in DE, (2) the share of electricity in the grid that was used by flexible consumers (electricity storage units, electrolyzers) in DE and (3) both shares aggregated as a metric to indicate the overall flexibility of the German electricity system. While all *el scenarios* produced more electricity from flexible generators, all H_2 scenarios were characterized by a higher combined flexibility. Most importantly, this extra flexibility was introduced into the system through the additional H_2 production from electrolyzers in the H_2 scenarios. In all cases, electrolyzers in the H_2 scenarios consumed 1.7 - 3.6 % more of grid electricity than in the respective *el scenarios*. While electricity consumption itself does not necessarily indicate that electrolyzers were used as flexible electricity consumers, the consistently medium FLH of electrolyzers clearly show that electrolyzers were selectively used in the German electricity system. And indeed, looking at the temporal production pattern of electrolyzers in DE shows a distinct diurnal H_2 production pattern with a strong peak in H_2 production during noon where PV electricity output is highest.

Interestingly, investing into additional electrolyzers in the H_2 scenario also resulted into much lower costs for the German electricity system than adding a similar flexibility to the system through H_2 gas power plants as in the *el scenarios*. This represents an important insight to explain why domestic H_2 production was still very high in the wind and PV constraint scenarios in DE, where electricity is a presumably scarce resource. Even in these scenarios, at least 16.8 % of the annual grid electricity was used for domestic H_2 production. The temporal production pattern of electrolyzers (Figure A.7) in DE further underlines this finding as average hourly H_2 production in DE followed a clear diurnal pattern in all scenarios with a strong peak in H_2 production during noon where PV electricity output is highest. Conversely, average H_2 production in AT only showed a distinct diurnal variation in the outlier scenarios, where exceptionally large PV capacities were installed. Altogether, this indicates that electrolyzers were important sources of demand-side flexibility in the German electricity system.

As another benefit, large electrolyzer capacities could also reduce grid expansion costs as they can provide more efficient and controllable demand-side management for the electricity system than other demand-side management options. Firstly, large-scale electrolyzers must be connected to high grid levels (i.e. large transmission lines with high voltage systems) and can therefore provide substantial demand-side flexibility at these levels.

⁸excluding output from battery and hydro storages

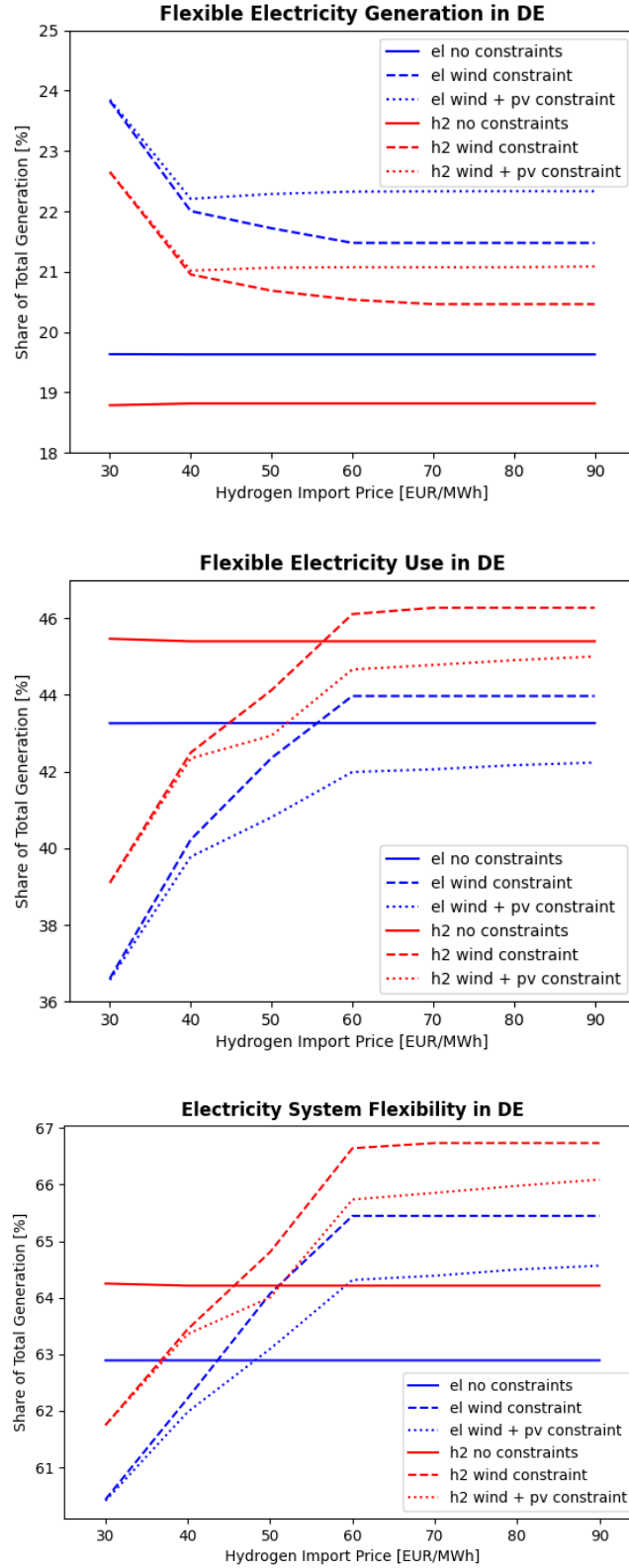


Figure 13: Calculated electricity system flexibilities in DE. Top: Share of flexible electricity generation from overall electricity fed into the grid; Middle: Share of flexible electricity consumption from overall electricity fed into the grid; Bottom: Aggregated shares of flexible electricity generation and consumption as an indicator of overall flexibility.

This potentially reduces the requirement to expand mid and low level grid infrastructure (like medium voltage transmission lines and distribution grids) to prepare the electricity grid for very high shares of intermittent renewable generation. In contrast, relying on large-scale demand-side management on low grid levels, for example through electric vehicles on a household scale, might require larger investments into mid and low grid level structures to transport intermittent renewable electricity from large generation plants (such as free-field PV plants and wind farms with typically more than 10 MW) to the consumer. Secondly, commercially operated electrolyzers are very likely easier to control as flexible consumers than private households since they better react to market incentives than the average private person. Accordingly, adequately designed market structure can allow to guide commercial electrolyzers to operate beneficially for the entire electricity system. In this way, electrolyzers might represent a way to easily control large-scale demand-side management and to reduce the required capacities of expensive and inefficient flexible electricity generators. Exploring the benefits of large-scale demand-side flexibility through electrolyzers could therefore represent an important field for future research to optimize grid expansion plans.

The benefits of electrolyzers as a source for flexibility in the electricity system are, however, limited to providing demand-side flexibility as they cannot stabilize the system at times of low renewable electricity generation. As this study further shows, batteries and H_2 gas power plants were needed in all scenarios in DE. While electrolyzers can "shave" large electricity peaks, batteries and H_2 power plants are indispensable to provide additional electricity at times when intermittent electricity generation is far too low to meet the base electricity demand. The no constraints scenarios show that such flexible electricity generators were also needed in DE even when wind and PV capacities could be expanded without limits. In AT, existing storage capacities were in most scenarios sufficient to provide sufficient flexible electricity generation.

6.3 H_2 Imports and Domestic H_2 Production

The results of this study further indicate that a H_2 import price of 60 €/MWh marks a threshold below which H_2 imports and the use of H_2 gas power plants become increasingly competitive while the economic benefits of domestic H_2 production diminish. Despite this economical competitiveness of H_2 imports below 60 €/MWh, it is highly uncertain whether H_2 import prices will actually fall below 60 €/MWh in the foreseeable future. Even though Brändle et al. (2021), for example, expect green H_2 production costs to drop below 1 USD/kg H_2 (approx. 28.2 €/MWh)⁹ in some regions with particularly good conditions for RE generation by 2050, they also estimate that H_2 import into DE cannot be realized below approximately 58 €/MWh¹⁰ in 2050. The reason for this large difference between local production costs and actual import costs are the high transport costs from shipping H_2 into Europe. As shipping typically adds more than 1 USD/kg (approx. 28.2 €/MWh) to the local H_2 production costs (Brändle et al., 2021), countries with ultra-low production costs for green H_2 will likely not be able to offer green H_2 below 60 €/MWh. Brändle et al. (2021) further expect that regions, from where H_2 could be imported via pipelines, will not be able to produce very cheap green H_2 .

6.4 Limitations

Altogether, the results of this study lie in a similar range of other studies on 100 % renewable electricity systems in AT and DE even though it is difficult to compare the results of this study with other studies due to different assumptions on energy generation and energy consumption. Compared to approx. 83 - 93 GW electrolyzer capacities, for example, Prognos, Öko-Institut and Wuppertal Institut (2021) estimated that 50 GW electrolyzer capacities were necessary for a climate neutral electricity system in DE, while a study by Stiftung Arbeit und Umwelt der IG BCE (2021) expects even more than 120 GW electrolyzers might be necessary for a high H_2 use in the German industry. Similarly, Prognos, Öko-Institut and Wuppertal Institut (2021) estimate over 70 GW of flexible generation capacity from renewable gases to be necessary in

⁹assuming 1 USD = 0.93 €, exchange rate on 13.02.2023

¹⁰assuming pipeline transport from Morocco

a climate neutral German electricity system compared to the 45.1 - 62.5 GW of flexible H_2 gas power plants estimated in this study, which did not include flexible biogas power plants. While Hansen et al. (2019) estimate between 1100 and 1300 TWh annual electricity generation in a 100 % renewable German electricity system, DE produced 1233 - 1400 TWh of electricity in this study. In AT, for example, Ramsebner and Haas (2021) estimate 4 GW electrolyzer capacity and 4.5 GW flexible gas capacities to be installed in a possible renewable Austrian electricity system. With 0 - 4.4 GW electrolyzers¹¹ and 0 - 1.7 GW H_2 power plants, this study even slightly underestimates the capacities from Ramsebner and Haas (2021). Only the outlier scenarios in the wind constraint scenarios in AT diverged considerably from other studies and the adjacent scenarios calculate different in this study.

The electrolyzer capacities calculated in this study might, however, also overestimate the economically ideal electrolyzer capacities as it did not consider the costs for necessary electricity and gas grid expansions for the implementation of such large grid-connected electrolyzer capacities. Furthermore, it ignores grid use fees that effectively increase the costs for grid connected H_2 production and impair the development of successful business cases for electrolyzer projects. As a result, lower domestic electrolyzer capacities might in fact be economically most efficient. In addition, the actually realized electrolyzer capacities might further be lower in a 100 % renewable electricity system than in an economically ideal system as system benefits (e.g. benefits of flexible electricity consumption) of electrolyzers might not be sufficiently passed to individual electrolyzers and therefore not be included into individual investment decisions. In particular in the German electricity system, this could become an important factor to build an economically efficient electricity system. Accordingly, market structures must ensure that individual electrolyzer projects can sufficiently profit from the benefits they introduce into the electricity system.

The results of this study are furthermore based on the assumption that *iron making* requires a constant energy demand and cannot flexibly adapt its energy consumption. Moreover, general electricity demand was assumed to be completely inelastic according to a given load profile. Consequently, the ability of consumers to flexibly use electricity might fundamentally change the results of this study depending on the degree of demand-side flexibility that can actually be achieved by these consumers. The results of this study can therefore not be generalized to all applications where H_2 and electricity compete as possible energy carriers. The present results also do not represent a forecast of the actual energy system in AT and DE in 2040. In particular, the finding of this study cannot be used to judge the electricity system effects of directly electrified applications that allow flexible electricity consumption, such as battery electric vehicles. For I & S production, further research should evaluate the potential system benefits of a large-scale demand-side management in steel production. This will in steel production, however, be limited by economic considerations as steel plant operators typically ensure that their plants run at highest possible capacity (Pimm et al., 2021). Therefore, another aspect of further research could investigate the business cases of individual steel plants with flexible energy consumption. In addition, the economic performance of iron ore electrolyzers represents a huge uncertainty on whether electricity-based *iron making* can be widely adopted in the industry at all. As this study shows, decisions on technically feasible steel production technologies should however always consider their effects on the underlying electricity system and grid infrastructure.

The findings of this study are further limited as the model results were based on only one year of historic renewable electricity generation data. Even though this year was chosen to represent an average or even below average year for renewable electricity generation, the data used in this study might underestimate times with low intermittent electricity generation (e.g. "dunkelflaute") and simultaneous high demand. In particular, if the mismatch between intermittent generation and actual consumption might in reality occur over a considerably longer time period than modelled in this study, blackouts are possible. Therefore, the results should not be considered as a representation of ideal electricity systems for the future. In order to plan safe electricity system for the future, further risk analysis must be conducted on extreme

¹¹excluding outlier scenarios

weather events that lead to a prolonged mismatch between intermittent electricity generation and consumption.

Finally, this study regarded the Austro-German electricity systems as completely independent from the European electricity grid. This limits the overall flexibility of the modelled system as renewable resources are more diversely distributed over the European continent. Consequently, a larger network of connected electricity systems is more stable at times where individual regions experience very poor conditions for intermittent renewable electricity generation. Modelling a wider European electricity system, however, also needs to be approached with care as the chosen modelling approach might also adversely influence the results. This could be seen in the exceptionally high PV and battery storage capacities in AT in the wind constraint scenario, where additional PV capacities from the overall system were solely installed in AT and none in DE as this produce the solution with the least overall costs. Models that include several subsystems and that are optimized for a global paramtere must therefore contain appropriate restrictions to prevent such unrealistic outcomes.

7 Conclusion

This study investigated the effects of directly and indirectly decarbonizing *iron making* in steel production through iron ore electrolysis or H_2 direct reduction on completely renewable electricity systems in AT and DE. For this purpose, the connected Austrian and German electricity systems were modelled with the power system model *medea* that allows to simulate tightly coupled electricity, H_2 and district heating systems. To evaluate the effects of different degrees of wind and PV expansion, three scenario lines were developed for each *iron making* technology: (1) the wind and PV constraint scenarios, where both wind an PV capacities were limited to the officially declared capacity targets; (2) the wind constraint scenarios, where only wind capacity was limited to the defined capacity target; and (3) the no constraint scenarios, where wind and PV capacities could be freely expanded by the model the reach an economic optimum. For each of these scenario lines, the full system was modelled assuming seven different H_2 import prices between 30 - 90 €/MWh to observe the effects different H_2 import prices on the system. Consequently, a total of 42 different scenarios were simulated in this study.

The results show marked differences between the Austrian and the German electricity system. In DE, electricity-powered *iron making* considerably increased system costs and gross energy consumption as the higher electricity demand from a directly electrified steel production increased the demand for expensive and inefficient H_2 gas power plants. In contrast, H_2 -based *iron making* decreased system costs and system gross electricity consumption as domestic electrolyzers could provide large-scale demand-side flexibility to the electricity system and thereby reduce the demand for expensive and inefficient H_2 gas power plants and other electricity storage units. Besides H_2 infrastructure, large short-term battery storage capacities were also required in DE to stabilize the modelled renewable electricity system. In AT, on the other hand, H_2 gas power plants and domestic electrolyzers were only deployed in some scenarios, indicating that they will likely not become essential elements of a 100 % renewable Austrian electricity system. The Austrian electricity system furthermore benefited from its large installed hydro storage capacities that were able to buffer most differences between electricity generation and demand. With these hydro storage capacities, a direct electrification of the Austrian steel industry improved the economic and energetic energy efficiency of a completely renewable Austrian electricity system. Even in scenarios with higher electricity demands, AT required only moderate battery storage capacities.

In addition, the results indicate that expanding renewable generation capacities beyond the already declared capacity targets will largely diminish the competitiveness of H_2 imports. While DE was able to domestically produce the majority of its H_2 demand in all scenarios, it did not import any H_2 above 60 €/MWh H_2 in scenarios where wind or PV capacities could be expanded beyond their capacity targets. Similarly, AT only imported H_2 above 60 €/MWh H_2 in the wind and PV constraint scenarios. Since it remains highly uncertain whether H_2 can

be imported for less than 60 €/MWh in the foreseeable future, domestic green H_2 production will likely be economically competitive in both AT and DE.

While this study only represents an exploratory study and therefore does not represent a forecast for the future electricity systems in AT and DE, it nevertheless provides valuable insights into the importance of demand-side and generation-side flexibility that should be considered for expansion plans of the Austrian and German electricity grids. In particular, it provides a strong argument for the importance of large-scale, flexibly-run electrolyzers for the German electricity system. Since individual electrolyzers operate to maximize their individual profits and not to minimize electricity system costs, future market designs for electrolyzers should ensure that the economic benefits of flexibly-run electrolyzer for the entire electricity system are passed to individual electrolyzer units. Finally, this study shows that the most energy efficient steel production technology does not necessarily represent the most energy efficient technology for the entire energy system. Accordingly, the system effects of new technologies for energy-intensive applications should always be considered for decisions on a sustainable transformation of such energy-intensive applications such as steel production.

References

- AG Energiebilanzen. (2021, April 6). Energiebilanz der Bundesrepublik Deutschland 2019. Retrieved May 11, 2022, from <https://ag-energiebilanzen.de/daten-und-fakten/bilanzen-1990-bis-2020/>
- Allanore, A., Lavelaine, H., Birat, J., Valentin, G., & Lapique, F. (2010). Experimental investigation of cell design for the electrolysis of iron oxide suspensions in alkaline electrolyte. *Journal of applied electrochemistry*, 40(11), 1957–1966. <https://doi.org/https://doi.org/10.1007/s10800-010-0172-0>
- Allanore, A., Yin, L., & Sadoway, D. R. (2013). A new anode material for oxygen evolution in molten oxide electrolysis. *Nature*, 497(7449), 353–356. <https://doi.org/https://doi.org/10.1038/nature12134>
- Bailera, M., Lisbona, P., Peña, B., & Romeo, L. M. (2021). A review on co2 mitigation in the iron and steel industry through power to x processes. *Journal of CO2 Utilization*, 46, 101456.
- Barberousse, M., Apostolou, M., Debregas, A., & Bono, C. (2020). Electrification of primary steel production based on iderwin process: Simulation on the european power system in 2050. Retrieved November 6, 2022, from https://www.eceee.org/library/conference_proceedings/eceee.Industrial_Summer_Study/2020/6-deep-decarbonisation-of-industry/electrification-of-primary-steel-production-based-on-iderwin-process-simulation-on-the-european-power-system-in-2050/
- Baumann, Martin and Pauritsch, Günter and Rohrer, Michael and Schweitzer, Marcel. (2022, July). Aktualisierung der Roadmap zur Dekarbonisierung der Fernwärme in Österreich. Retrieved November 20, 2022, from https://www.gaswaerme.at/media/medialibrary/2022/11/FGW-Roadmap2-Endbericht-Final_2022-11-07.pdf
- Bhaskar, A., Assadi, M., & Nikpey Somehsaraei, H. (2020). Decarbonization of the iron and steel industry with direct reduction of iron ore with green hydrogen. *Energies*, 13(3), 758.
- Biermayr, P., Dißauer, C., Eberl, M., Enigl, M., Fechner, H., Fürsinn, B., Jaksch-Fliegenschnee, M., Leonhartsberger, K., Moidl, S., Prem, E., Savic, S., Schmidl, C., Strasser, C., Weiss, W., Wittmann, M., Wonisch, P., & Wopienka, E. (2022). Innovative Energietechnologien in Österreich Marktentwicklung 2021 [Studie im Auftrag des Bundesministerium für Klimaschutz, Umwelt, Energie, Mobilität, Innovation und Technologie (BMK)]. Retrieved November 20, 2022, from <https://nachhaltigwirtschaften.at/resources/iea.pdf/schriftenreihe-2022-21b-marktstatistik-2021-web.pdf>
- BMK. (2022). Wasserstoffstrategie für österreich. Retrieved November 6, 2022, from <https://www.bmk.gv.at/themen/energie/energieversorgung/wasserstoff/strategie.html>
- BMWK. (2020). Die nationale wasserstoffstrategie. Retrieved November 6, 2022, from <https://www.bmwk.de/Redaktion/DE/Publikationen/Energie/die-nationale-wasserstoffstrategie.html>
- Boston Metals. (2022a). Benefits of our technology. Retrieved December 1, 2022, from <https://www.bostonmetal.com/benefits-of-moe/>
- Boston Metals. (2022b). Transforming metal production. Retrieved December 1, 2022, from <https://www.bostonmetal.com/transforming-metal-production/>
- Brändle, G., Schönfisch, M., & Schulte, S. (2021). Estimating long-term global supply costs for low-carbon hydrogen. *Applied Energy*, 302, 117481. <https://doi.org/https://doi.org/10.1016/j.apenergy.2021.117481>
- Büttner, S. (2023). Medea_decarbonizing_steel_industry [GitHub repository]. https://github.com/simobu/medea_decarbonizing_steel_industry
- Cavaliere, P. (2019). Electrolysis of iron ores: Most efficient technologies for greenhouse emissions abatement. *Clean ironmaking and steelmaking processes* (pp. 555–576). Springer.
- Danish Energy Agency. (2020). Datasheet for energy storage. Retrieved October 20, 2022, from <https://ens.dk/en/our-services/projections-and-models/technology-data/technology-data-energy-storage>

- Danish Energy Agency. (2022a). Data sheet for electricity and district heat production - updated june 2022. Retrieved October 20, 2022, from <https://ens.dk/en/our-services/projections-and-models/technology-data/technology-data-generation-electricity-and>
- Danish Energy Agency. (2022b). Data Sheets for energy carrier generation and conversion. Retrieved October 20, 2022, from <https://ens.dk/en/our-services/projections-and-models/technology-data/technology-data-renewable-fuels>
- Deutscher Bundestag. (2022a). Gesetz zu Sofortmaßnahmen für einen beschleunigten Ausbau der erneuerbaren Energien und weiteren Maßnahmen im Stromsektor. Retrieved September 14, 2022, from https://www.bgbl.de/xaver/bgbl/start.xav#_bgbl_%2F%2F*%5B%40attr_id%3D%27bgbl122s1237.pdf%27%5D__1663161874821
- Deutscher Bundestag. (2022b). Zweites Gesetz zur Änderung des Windenergie-auf-See-Gesetzes und anderer Vorschriften. Retrieved September 14, 2022, from https://www.bgbl.de/xaver/bgbl/start.xav#_bgbl_%2F%2F*%5B%40attr_id%3D%27bgbl122s1325.pdf%27%5D__1663164977760
- E-Control. (2022). E-control statistikbroschüre 2022 - berichtsjahr 2021. Retrieved April 30, 2023, from <https://www.e-control.at/publikationen/statistik-bericht>
- ENTSO-E. (n.d.). Installed capacity per production type [entso-e transparency platform]. Retrieved November 20, 2022, from <https://transparency.entsoe.eu/generation/r2/installedGenerationCapacityAggregation/show>
- ENTSO-E. (2022). Demand time series 2040 distributed energy [data set]. Retrieved October 1, 2022, from <https://2022.entsoe-tyndp-scenarios.eu/download/>
- ENTSO-E, & ENTSG. (2022). Tyndp 2022: Scenario report. Retrieved October 1, 2022, from <https://2022.entsoe-tyndp-scenarios.eu/>
- Fan, Z., & Friedmann, S. J. (2021). Low-carbon production of iron and steel: Technology options, economic assessment, and policy. *Joule*, 5(4), 829–862.
- Fischedick, M., Marzinkowski, J., Winzer, P., & Weigel, M. (2014). Techno-economic evaluation of innovative steel production technologies. *Journal of Cleaner Production*, 84, 563–580.
- Fraunhofer ISI, Fraunhofer ISE, & Fraunhofer IEG. (2021). Metastudie wasserstoff – auswertung von energiesystemstudien. Retrieved November 6, 2022, from https://www.isi.fraunhofer.de/de/competence-center/energiotechnologien-energiesysteme/projekte/Metastudie.Wasserstoff_Abschlussbericht.html
- Gielen, D., Saygin, D., Taibi, E., & Birat, J.-P. (2020). Renewables-based decarbonization and relocation of iron and steel making: A case study. *Journal of Industrial Ecology*, 24(5), 1113–1125.
- Hamadeh, H., Mirgaux, O., & Patisson, F. (2018). Detailed modeling of the direct reduction of iron ore in a shaft furnace. *Materials*, 11(10). <https://doi.org/10.3390/ma11101865>
- Hansen, K., Mathiesen, B. V., & Skov, I. R. (2019). Full energy system transition towards 100 % renewable energy in germany in 2050. *Renewable and Sustainable Energy Reviews*, 102, 1–13. <https://doi.org/https://doi.org/10.1016/j.rser.2018.11.038>
- Harpprecht, C., Naegler, T., Steubing, B., Tukker, A., & Simon, S. (2022). Decarbonization scenarios for the iron and steel industry in context of a sectoral carbon budget: Germany as a case study. *Journal of Cleaner Production*, 134846. <https://doi.org/https://doi.org/10.1016/j.jclepro.2022.134846>
- Hay, T., Visuri, V.-V., Aula, M., & Echterhof, T. (2021). A review of mathematical process models for the electric arc furnace process. *steel research international*, 92(3), 2000395.
- Hegemann, K.-R., & Guder, R. (2019). *Roheisenerzeugung*. Springer Vieweg. <https://doi.org/10.1007/978-3-658-25406-3>
- Hegemann, K.-R., & Guder, R. (2020). *Stahlerzeugung*. Springer Vieweg. <https://doi.org/10.1007/978-3-658-29091-7>
- IEA. (2020). Iron and Steel Technology Roadmap – Analysis. Retrieved June 6, 2022, from <https://www.iea.org/reports/iron-and-steel-technology-roadmap>
- IEA. (2021). Global hydrogen review 2021. Retrieved June 2, 2022, from <https://www.iea.org/reports/global-hydrogen-review-2021>
- Keuneke, R. (2019). Wasserkraft in deutschland – aktuelle zahlen und entwicklung. *Wasserwirtschaft*, 5, 138–141. <https://www.floecksmuehle-fwt.de/userfiles/fileadmin-ibfm/>

- Kim, J., Sovacool, B. K., Bazilian, M., Griffiths, S., Lee, J., Yang, M., & Lee, J. (2022). Decarbonizing the iron and steel industry: A systematic review of sociotechnical systems, technological innovations, and policy options. *Energy Research & Social Science*, 89, 102565.
- Krutzler, T., Wiesenberger, H., Heller, C., Gössl, M., Stranner, G., Storch, A., Heinfellner, H., Winter, R., Kellner, M., & Schindler, I. (2016). Szenario erneuerbare energie 2030 und 2050 [Publikation des Umweltbundesamts im Auftrag des Österreichischen Biomasseverbandes, IG Windkraft und save energy Austria]. Retrieved November 20, 2022, from <https://www.umweltbundesamt.at/fileadmin/site/publikationen/REP0576.pdf>
- Kushnir, D., Hansen, T., Vogl, V., & Åhman, M. (2020). Adopting hydrogen direct reduction for the swedish steel industry: A technological innovation system (tis) study. *Journal of Cleaner Production*, 242, 118185. <https://doi.org/https://doi.org/10.1016/j.jclepro.2019.118185>
- Lechtenböhrer, S., Nilsson, L. J., Åhman, M., & Schneider, C. (2016). Decarbonising the energy intensive basic materials industry through electrification—implications for future eu electricity demand. *Energy*, 115, 1623–1631. <https://doi.org/https://doi.org/10.1016/j.energy.2016.07.110>
- Mayer, J., Bachner, G., & Steininger, K. W. (2019). Macroeconomic implications of switching to process-emission-free iron and steel production in europe. *Journal of Cleaner Production*, 210, 1517–1533.
- Mousa, E. (2019). Modern blast furnace ironmaking technology: Potentials to meet the demand of high hot metal production and lower energy consumption. *Metallurgical and Materials Engineering*, 25(2), 69–104. <https://doi.org/https://doi.org/10.30544/414>
- Öberg, S., Odenberger, M., & Johnsson, F. (2022). Exploring the competitiveness of hydrogen-fueled gas turbines in future energy systems. *International Journal of Hydrogen Energy*, 47(1), 624–644. <https://doi.org/https://doi.org/10.1016/j.ijhydene.2021.10.035>
- OECD. (2022). Producer price indices (ppi) (indicator). <https://doi.org/10.1787/a24f6fa9-en>
- Österreichischer Nationalrat. (2021). Erneuerbaren-Ausbau-Gesetz - EAG. <https://www.ris.bka.gv.at/GeltendeFassung.wxe?Abfrage=Bundesnormen&Gesetzesnummer=20011619>
- Pei, M., Petäjäniemi, M., Regnell, A., & Wijk, O. (2020). Toward a fossil free future with hybrit: Development of iron and steelmaking technology in sweden and finland. *Metals*, 10(7), 972.
- Pimm, A. J., Cockerill, T. T., & Gale, W. F. (2021). Energy system requirements of fossil-free steelmaking using hydrogen direct reduction. *Journal of Cleaner Production*, 312, 127665.
- Prognos, Öko-Institut and Wuppertal Institut. (2021). Klimaneutrales Deutschland: In drei Schritten zu null Treibhausgasen bis 2050 über ein Zwischenziel von -65 % im Jahr 2030 als Teil des EU-Green-Deals [Studie im Auftrag von Agora Energiewende, Agora Verkehrswende und Stiftung Klimaneutralität]. Retrieved November 20, 2022, from <https://www.agora-energiewende.de/veroeffentlichungen/klimaneutrales-deutschland/>
- Pye, S., Welsby, D., McDowall, W., Reinauer, T., Dessens, O., Winning, M., Calzadilla, A., & Bataille, C. (2022). Regional uptake of direct reduction iron production using hydrogen under climate policy. *Energy and Climate Change*, 100087. <https://doi.org/https://doi.org/10.1016/j.egycc.2022.100087>
- Ramsebner, J., & Haas, R. (2021). *Perspektiven der Sektorkopplung in Form von P2G für österreich bis 2030/2040 aus energiewirtschaftlicher Sicht* (tech. rep.). TU Wien & BMK. Retrieved April 27, 2022, from <https://www.bmk.gv.at/themen/energie/publikationen/sektorkoppelung.html>
- Schröder, A., Kunz, F., Meiss, J., Mendelevitch, R., & von Hirschhausen, C. (2013). Current and prospective costs of electricity generation until 2050. Retrieved December 19, 2022, from https://www.diw.de/documents/publikationen/73/diw_01.c.424566.de/diw_datadoc_2013-068.pdf

- Spanlang, A., Wukovits, W., & Weiss, B. (2016). Development of a blast furnace model with thermodynamic process depiction by means of the rist operating diagram. *Chemical Engineering Transactions*, 52, 973–978. <https://doi.org/https://doi.org/10.3303/CET1652163>
- Statistik Austria. (2022). Energiebilanz österreich 1970-2020. Retrieved April 24, 2022, from <https://www.statistik.at/statistiken/energie-und-umwelt/energie/energiebilanzen>
- Stiftung Arbeit und Umwelt der IG BCE. (2021). Wasserstoffbasierte industrie in deutschland und europa. Retrieved November 6, 2022, from <https://enervis.de/leistung/wasserstoffbasierte-industrie-in-deutschland-und-europa/>
- Toktarova, A., Walter, V., Göransson, L., & Johnsson, F. (2022). Interaction between electrified steel production and the north european electricity system. *Applied Energy*, 310, 118584.
- Umweltbundesamt. (2022). Zeitreihen zur entwicklung der erneuerbaren energien in deutschland [Daten der Arbeitsgruppe Erneuerbare-Energie Statistiken]. Retrieved November 21, 2022, from <https://www.erneuerbare-energien.de/EE/Navigation/DE/Service/Erneuerbare.Energien.in.Zahlen/Zeitreihen/zeitreihen.html>
- Venkataraman, M., Csereklyei, Z., Aisbett, E., Rahbari, A., Jotzo, F., Lord, M., & Pye, J. (2022). Zero-carbon steel production: The opportunities and role for australia. *Energy Policy*, 163, 112811.
- Victoria, M., Zeyen, E., & Brown, T. (2022). Speed of technological transformations required in europe to achieve different climate goals. *Joule*, 6(5), 1066–1086. <https://doi.org/https://doi.org/10.1016/j.joule.2022.04.016>
- Vogl, V., Åhman, M., & Nilsson, L. J. (2018). Assessment of hydrogen direct reduction for fossil-free steelmaking. *Journal of cleaner production*, 203, 736–745. <https://doi.org/https://doi.org/10.1016/j.jclepro.2018.08.279>
- Wehrle, S., Gruber, K., & Schmidt, J. (2021). The cost of undisturbed landscapes. *Energy Policy*, 159, 112617. <https://doi.org/10.1016/j.enpol.2021.112617>
- West, K. (2020). High-temperature molten oxide electrolysis steelmaking (ulcolysis) [Fact-sheet]. Retrieved November 21, 2022, from https://energy.nl/media/data/Ulcolysis-Technology-Factsheet_080920.pdf
- Wiencke, J., Lavelaine, H., Panteix, P.-J., Petitjean, C., & Rapin, C. (2018). Electrolysis of iron in a molten oxide electrolyte. *Journal of Applied Electrochemistry*, 48(1), 115–126. <https://doi.org/https://doi.org/10.1007/s10800-017-1143-5>
- World Steel Association. (2022). Annual production steel data. Retrieved November 2, 2022, from <https://worldsteel.org/steel-by-topic/statistics/annual-production-steel-data/>

A Figures

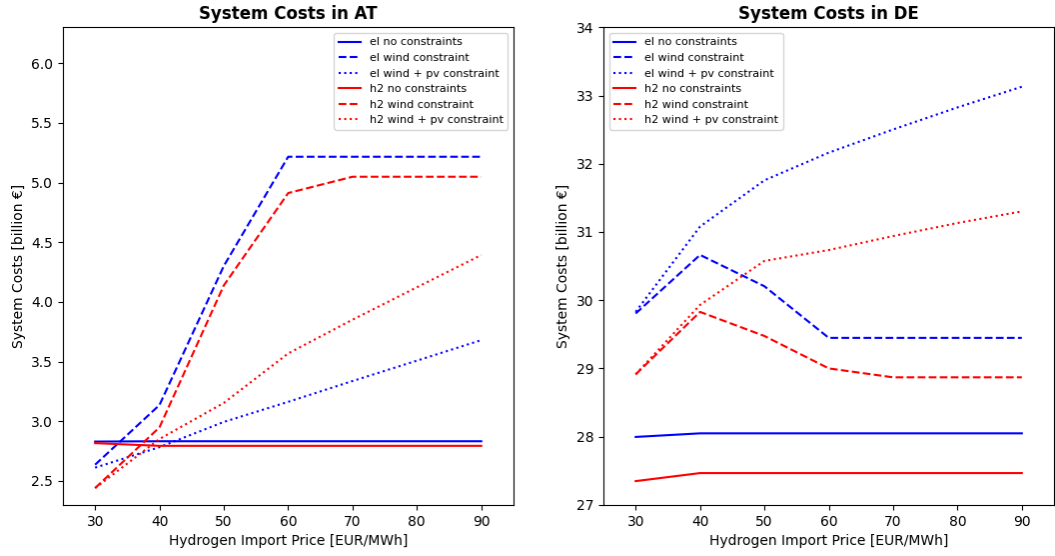


Figure A.1: System costs in each country. Note that *medea* minimizes system costs for the overall system and not for each individual country.

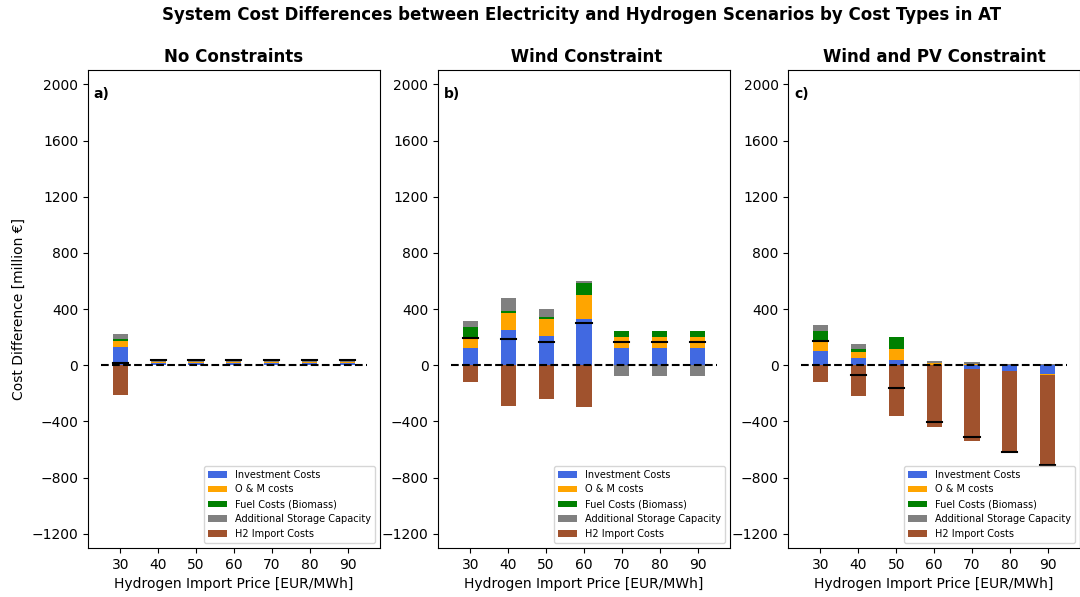


Figure A.2: Cost differences between *el* scenarios and *H₂* scenarios in AT. The numbers solely represent cost differences and not total costs. Positive values indicate higher costs in the *el* scenarios while negative costs indicate higher costs in the *H₂* scenario.

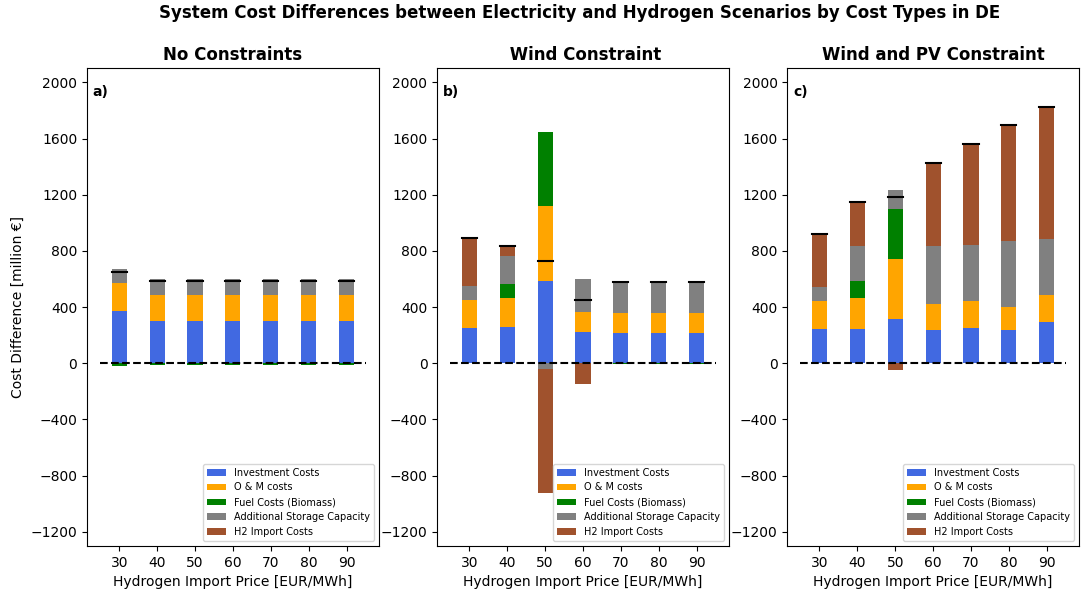


Figure A.3: Cost differences between *el scenarios* and H_2 scenarios in DE. The numbers solely represent cost differences and not total costs. Positive values indicate higher costs in the *el scenarios* while negative costs indicate higher costs in the H_2 scenario.

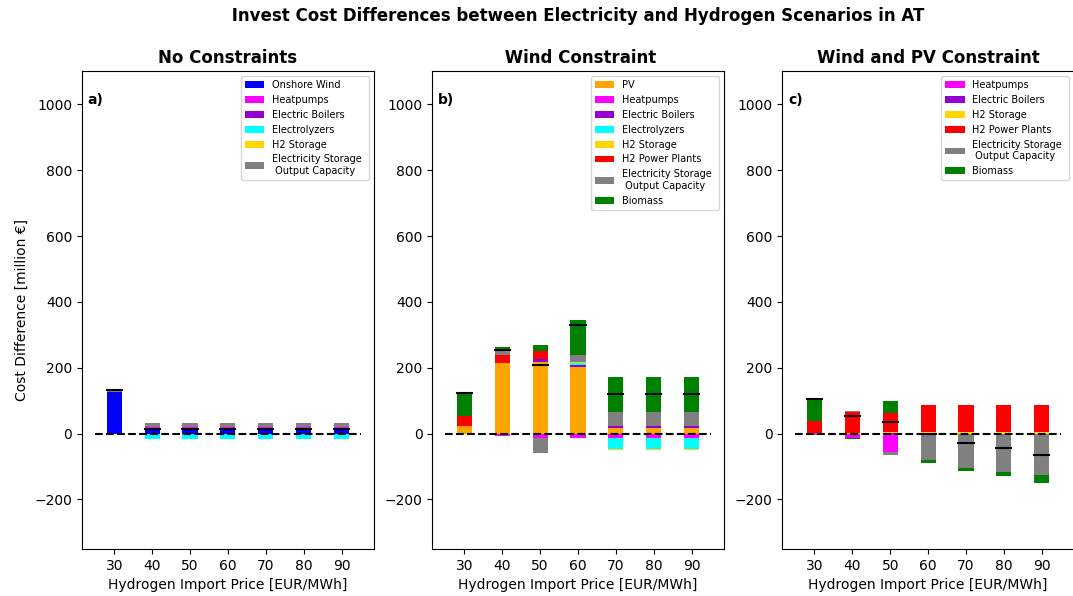


Figure A.4: Investment cost differences between *el scenarios* and H_2 scenarios in AT. The numbers solely represent cost differences and not total costs. Positive values indicate higher costs in the *el scenarios* while negative costs indicate higher costs in the H_2 scenario.

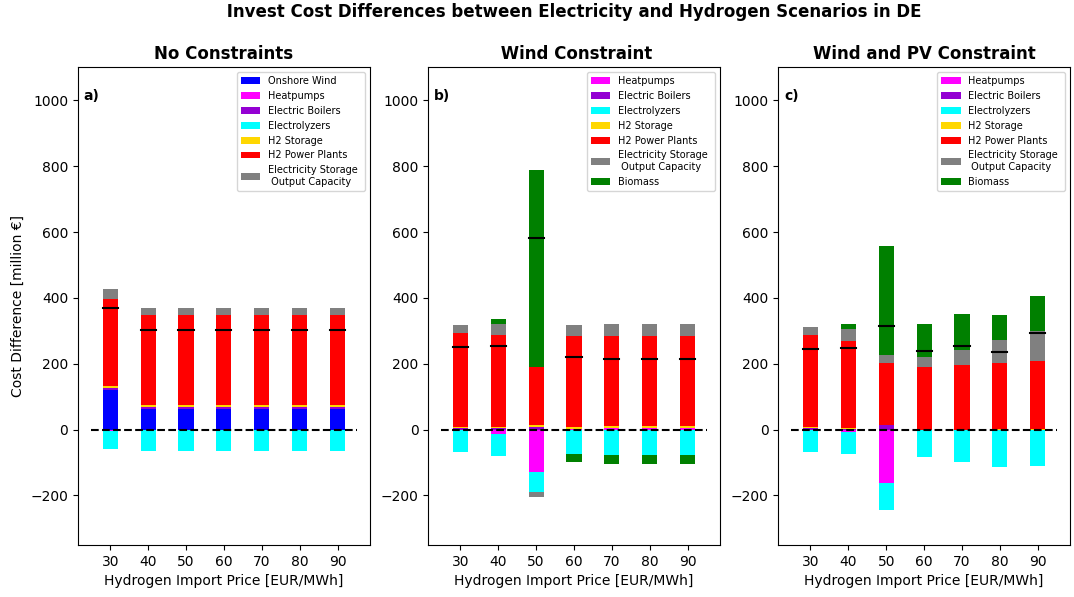


Figure A.5: Investment cost differences between *el scenarios* and *H₂ scenarios* in DE. The numbers solely represent cost differences and not total costs. Positive values indicate higher costs in the *el scenarios* while negative costs indicate higher costs in the *H₂ scenario*.

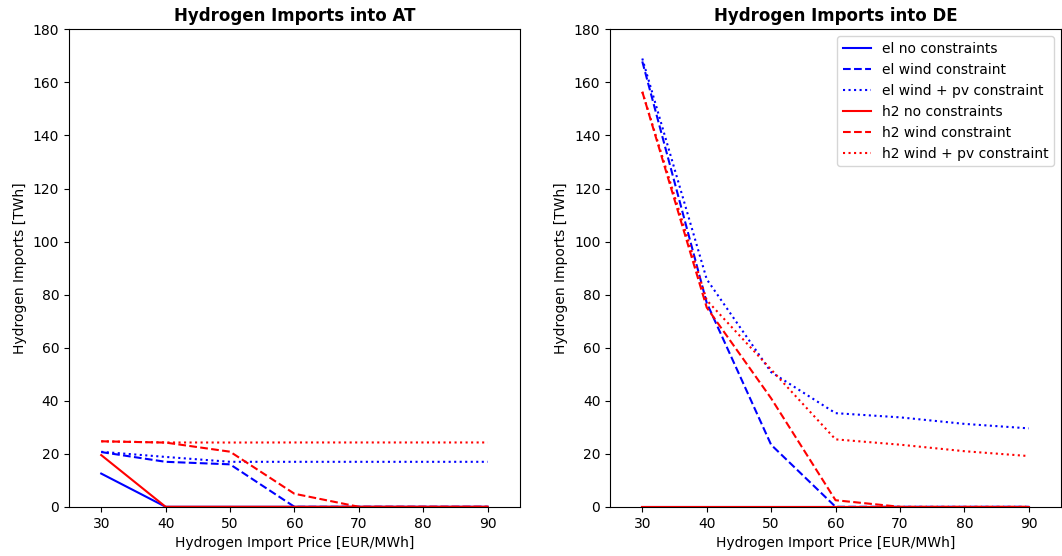


Figure A.6: Annual hydrogen imports into AT (left) and DE (right).

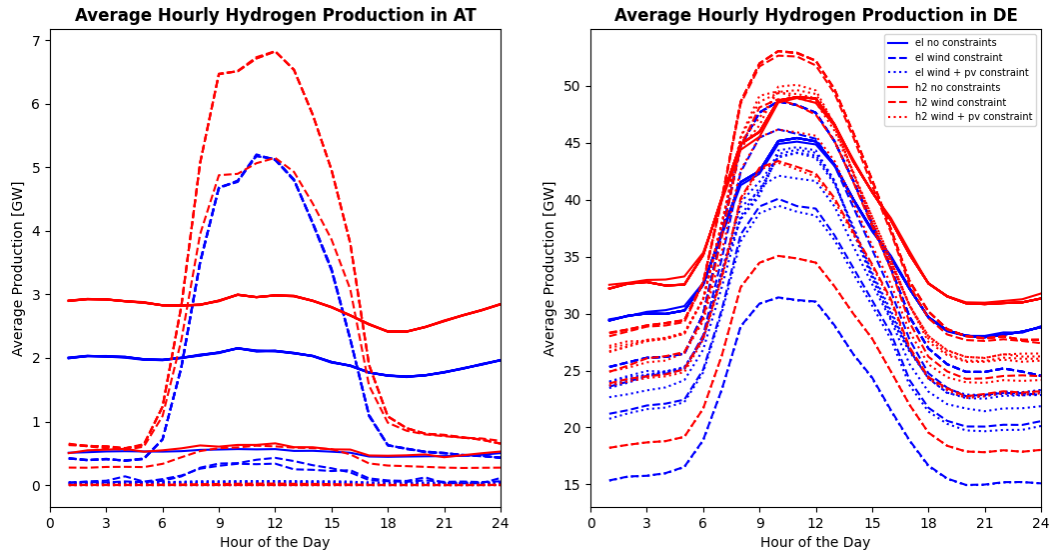


Figure A.7: Average hourly H_2 production over the course of one day. Note that each calculated scenario represent one line, i.e. 42 lines are shown per country. The author is aware that averaging production over a typical day can only capture variations due to an adaptation of production patterns to the availability of PV electricity. If electrolyzers would only produce H_2 when wind electricity is available and not be affected by the availability of PV electricity, the graph above would likely show only flat curves.

Table 4: Technology data used as input for the model in this study

	Invest Costs	Storage Capacity Costs	Fixed O&M	Variable O & M	conversion efficiency	round trip efficiency	lifetime	Sources
unit	€/kW	€/kWh	€/kW	€/MWh	%	%	years	
PV	510	-	9	-	-	-	40	[1]
Run-of-river	-	-	66	-	-	-	60	[3]
Wind Onshore	997	-	12	1	-	-	30	[1]
Wind Offshore	1,680	-	34	3	-	-	30	[1]
Biomass	3,286	-	94	4	30	-	25	[1]
Biomass CHP	3,459	-	99	4	30	-	25	[1]
Biomass Boiler	427	-	34	3	95	-	25	[1]
Heatpump Compression	773	-	2	2	390	-	25	[1]
Heatpump Absorption	493	-	2	1	174	-	25	[1]
Electric Boiler	61	-	1	1	99	-	20	[1]
Battery (Li-Ion)	224	96	1	2	96	92	30	[2]
Hydro - Reservoir Storage	2,442	-	22	3	90	81	60	[4]
Hydro - Pumped Storage	3,052	-	22	3	90	81	60	[4]
SOEC Electrolyzer (1 MW)	1,342	-	161	-	82	-	20	[5]
AEC Electrolyzer (100 MW)	300	-	6	-	71.5	-	32	[5]
H2 - Cavern Storage	50	2	0	15 /TWh	99	98	100	based on [2]
Fuel Cell	966	-	48	0	50	-	10	[1]
H2 Power Plant	953	-	27	4	62	-	25	[1],[6]
H2 CHP Power Plant	1,001	-	29	4	62	-	25	[1],[6]
Hot Water Tank	-	3	1	0	98	96	50	[2]

Literature: [1] Danish Energy Agency (2022a); [2] Danish Energy Agency (2020); [3] Schröder et al. (2013); [4] Wehrle et al. (2021); [5] Danish Energy Agency (2022b); [6] Öberg et al. (2022)

Notes: All money values were converted to 2020€ using the producer price index (total market) for the Euro area from OECD (2022). PV costs were aggregated assuming 50 % free field and 50 % rooftop PV. H_2 cavern storage costs were based on the available estimate for "underground storage of gas" costs. Costs for H_2 gas turbines were estimated as the costs for NG gas turbines plus 15 % (Öberg et al., 2022). H_2 fired CHP plants were assumed to be 5 % more expensive than regular H_2 gas power plants.

B Notes

Diese Masterarbeit wurde entsprechend der "Regeln der guten wissenschaftlichen Praxis" der Universität Wien erstellt. Zudem hat der Autor sich bemüht die Bildrechte sämtlicher verwendeter externer Quellen zu achten und die Zustimmung zur Verwendung der Bilder in dieser Arbeit einzuholen. Sollte dennoch eine Urheberrechtsverletzung bekannt werden, ersuche ich um Meldung bei mir.